

RD-R169 134

PEAK-FLUX-DENSITY SPECTRA OF LARGE RADIO BURSTS AND
PROTON EMISSION FROM FLARES(U) AIR FORCE GEOPHYSICS LAB
HANSOM AFB MA E W OLIVER ET AL. 19 AUG 85

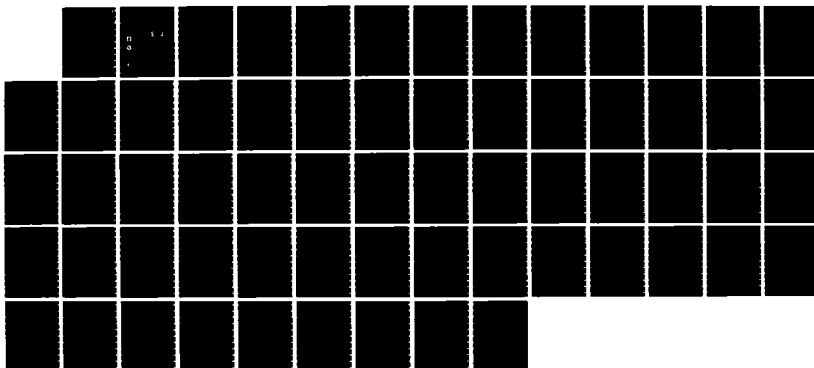
1/1

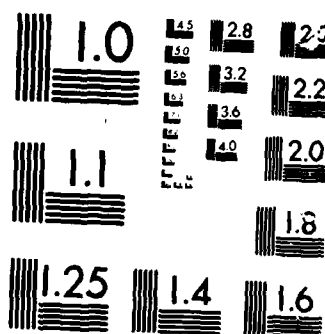
UNCLASSIFIED

AFGL-TR-85-0180

F/G 3/2

ML





MICROCOM[®]

CHART

AD-A169 134

(2)

AFGL-TR-85-0180
ENVIRONMENTAL RESEARCH PAPERS, NO. 924

Peak-Flux-Density Spectra of Large Solar Radio Bursts and Proton Emission From Flares

E. W. CLIVER
L. F. McNAMARA
L. C. GENTILE



19 August 1985



Approved for public release; distribution unlimited.



DTIC FILE COPY



SPACE PHYSICS DIVISION

PROJECT 2311

AIR FORCE GEOPHYSICS LABORATORY

HANSCOM AFB, MA 01731

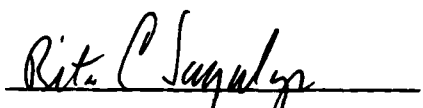
88 7 1 078

This technical report has been reviewed and is approved for publication.

FOR THE COMMANDER



E.G. MULLEN, Chief
Space Particles Environment Branch
Space Physics Division



RITA C. SAGALYN, Director
Space Physics Division

This document has been reviewed by the ESD Public Affairs Office (PA) and is releasable to the National Technical Information Service (NTIS).

Qualified requestors may obtain additional copies from the Defense Technical Information Center. All others should apply to the National Technical Information Service.

If your address has changed, or if you wish to be removed from the mailing list, or if the addressee is no longer employed by your organization, please notify AFGL/DAA, Hanscom AFB, MA 01731. This will assist us in maintaining a current mailing list.

UNCLASSIFIED

~~SECURITY CLASSIFICATION OF THIS PAGE~~

UNCLASSIFIED

SECURITY CLASSIFICATION OF THIS PAGE

19. ABSTRACT (Contd)

(33 percent). These statistics affirm various lines of evidence linking coronal shock waves and interplanetary proton events. They also suggest that the meter wavelength branch of the U-shaped spectrum may be attributable to second phase (vs flash phase) accelerated electrons. We have examined this latter supposition and find that it cannot be true in general, because for only about half of the bursts with the U-shaped spectrum (U-bursts) in our sample was a Type II in progress at the time of the peak of the low frequency branch. For these events one cannot rule out a possible contribution to the peak 200-MHz flux from either the second harmonic of the Type II burst or from flare continuum of the type FC II, provided that the starting frequency of the fundamental Type II burst is ≥ 100 MHz. The low frequency branch of the U-burst appears to be more closely related to impulsive phase Type III emission. We note that the small sample of U-bursts that lacked Type II/IV association is also poorly associated with proton events, and conclude that the observed association between U-bursts and proton events probably results from the Big Flare Syndrome rather than a close physical link between these two phenomena.

If the current NOAA prediction threshold of $J (> 10 \text{ MeV}) \geq 10 \text{ pr cm}^{-2} \text{ sec}^{-1} \text{ sr}^{-1}$ had been in effect during the period covered by our data base (1965 - 1979), the U-burst "yes or no" forecast tool would have had a false alarm rate of 50 to 70 percent and would have failed to provide warning for 40 to 50 percent of the significant prompt proton events attributable to disk flares. We note that several (8 of 46) of the prompt proton events with $J (> 10 \text{ MeV}) \geq 10 \text{ pr cm}^{-2} \text{ sec}^{-1} \text{ sr}^{-1}$ observed from 1965 to 1979 originated in flares that had relatively weak (≤ 300 sfu) burst emission at 200 MHz.

UNCLASSIFIED

SECURITY CLASSIFICATION OF THIS PAGE

Preface

A shorter version of this study has been published in the Journal of Geophysical Research, July 1, 1985, Vol. 90, pp. 6251-6266 (AFGL-TR-85-0176). The tables of events omitted from the JGR paper have been included in this report. We thank R. E. McGuire for providing proton data plots and S. W. Kahler and M. A. Shea for critical readings of the manuscript. We are grateful to A. Novak for typing and editing assistance.

Accession For	
NTIS CRA&I	<input checked="" type="checkbox"/>
DTIC TAB	<input type="checkbox"/>
Unannounced	<input type="checkbox"/>
Justification	
By _____	
Distribution /	
Availability Codes	
Dist	AVAIL. PUBL. OR SPL. STOR
A-1	



Contents

1. INTRODUCTION	1
2. RADIO AND PROTON DATA (1965-1979)	6
2.1 Radio Data Sources	6
2.2 Selection Criteria	6
2.3 Constructing Spectra	7
2.4 Spectral Classes	16
2.5 Associated Sweep Frequency Meter Wavelength Events	24
2.6 Proton Data	28
2.7 Major Proton Events, 1965-1979	30
3. DATA ANALYSIS	32
3.1 Peak-Flux-Density Spectral Type vs Proton Events	32
3.2 The U-Burst as a Forecast Tool	34
3.3 Radio Signatures of Major Proton Events	37
3.4 Microwave Spectral Class and Type II/IV Bursts	40
3.5 Timing of Type II Burst and 200-MHz Peak	43
4. DISCUSSION	45
4.1 Summary	45
4.2 The U-Burst as a Prediction Tool	46
4.3 The Low Frequency Branch of the U-Shaped Spectrum	47
4.4 U-Bursts and the Big Flare Syndrome	48
4.5 Impulsive Phase Proton Acceleration	48
4.6 Proton Flares With Weak 200-MHz Emission	49
REFERENCES	50

Illustrations

1. Examples of the Classic U-Shaped Spectrum, With the Low Frequency Maximum Occurring Near 200 MHz	17
2. Examples of the Classic U-Shaped Spectrum With the Low Frequency Maximum Occurring Near 200 MHz	18
3. Examples of U-Shaped Peak-Flux-Density Spectra That Had Their Lower Frequency Maximum in the Decimetric Range	19
4. Examples of U-Shaped Peak-Flux-Density Spectra That Had Their Lower Frequency Maximum in the Decimetric Range	20
5. Four of the Ten Events in Table 1 That Were Classified as U-Bursts Because of Our Decision to Favor High Flux Values at 200 MHz	21
6. The Timing of the Maximum \sim 200-MHz Emission for the U-Bursts in Table 1 Relative to the Timing of the \sim 10-GHz Maximum	22
7. Examples of Microwave Bursts With What We Have Termed "Intermediate" Peak-Flux-Density Spectra	25
8. Examples of Large Microwave Bursts With Cutoff or Quasi-Cutoff Spectra	26
9. Examples of Large Microwave Bursts With Cutoff or Quasi-Cutoff Spectra	27
10. Histograms of the Longitudinal Distributions of the H α Flares Associated With the Large Microwave Bursts in Table 1 Distributed According to Spectral Classification: (a) U-Shaped, (b) Intermediate, and (c) Cutoff	35
11. Histogram of the Reported Peak-Flux Density at \sim 200 MHz for the Parent Flares of the Large [$J (> 10 \text{ MeV}) \geq 10 \text{ pr cm}^{-2} \text{ sec}^{-1} \text{ sr}^{-1}$] Prompt Proton Events in Table 2 That Were Observed From 1965 to 1979	37
12. Histograms of the Durations of (a) Type II and (b) Type IV Emission for the Largest [$J (> 10 \text{ MeV}) \geq 10 \text{ pr cm}^{-2} \text{ sec}^{-1} \text{ sr}^{-1}$] Disk Flare ($85^\circ\text{E} \geq \phi \leq 85^\circ\text{W}$) Associated Prompt Proton Events That Occurred From 1965 to 1979	40

Tables

1. Large Microwave Bursts 1965-1979: Peak-Flux-Density Spectra, and Sweep Frequency Burst and Proton Association	8
2. Large Proton Events 1965-1979 With Unambiguous Visible-Disk-Flare Associations	31
3. Peak-Flux-Density Spectral Class vs Proton Event Size	33
4. Association of Sweep Frequency Bursts and Proton Events With Peak-Flux-Density Spectral Classes	41

Peak-Flux-Density Spectra of Large Solar Radio Bursts and Proton Emission From Flares

I. INTRODUCTION

Castelli et al¹ proposed that the "U-shaped" peak-flux-density radio spectrum, with high flux densities [$\gtrsim 1000$ solar flux units ($1 \text{ sfu} = 10^{-22} \text{ W m}^{-2} \text{ Hz}^{-1}$)] at meter and centimeter wavelengths and a minimum in the decimeter range, is the "preferred spectrum" for major solar proton flares. This concept was investigated in a series of papers by Castelli and his co-workers.²⁻⁶ In the initial reports on this topic,^{1,2} evidence was presented indicating that the U-shaped spectrum was a necessary or almost-necessary condition for a solar flare to produce a polar cap absorption (PCA) event. Thus, Castelli et al¹ found U-shaped radio spectra for the three visible hemisphere PCA flares of 1966.

In a verification of the utility of the U-shaped spectrum, O'Brien³ compiled a comprehensive list of 30 microwave events with this spectral shape (U-bursts) from observations reported by Sagamore Hill, Manila, Nagoya, and Pennsylvania State University from 1966 to 1968. He associated 13 of these flare-bursts with principal (≥ 2.0 dB of absorption measured by a 30-MHz riometer) PCA events and 14 with minor (< 2.0 dB) PCAs or with proton events detected only by satellites, but was unable to associate the three remaining U-bursts with a near-Earth

(Received for Publication 12 August 1985)

References 1 to 6 will not be listed here. See References, page 50.

particle enhancement. Significantly, in the reverse association, O'Brien found no cases of principal PCAs during this period that were not associated with U-bursts. Castelli and Barron⁵ compiled a comprehensive list of 81 U-bursts from 1966 to 1976. For nine of these events, a major proton event (PCA) was in progress at the time of the U-burst and no fresh injection of protons was observed. Seventy of the remaining 72 events were associated either with PCAs (27 of which had peak absorption ≥ 2.0 dB) or satellite proton events. For the same period, 1966 to 1976, Castelli and Tarnstrom⁶ published a catalog of 114 proton events that were associated with flares that did not have U-shaped microwave spectra. Seventy-six of these events could be identified with visible hemisphere flares, and, of these, only three were principal PCA events. Thus the current picture of the relationship between U-bursts and proton events is that the U-shaped spectrum is: (1) an almost sufficient condition ($70/72 = 97$ percent) for the occurrence of an interplanetary proton event of any size, and (2) an almost necessary condition ($27/30 = 90$ percent) for a principal PCA (≥ 2.0 dB) to occur.

Largely as a result of the efforts of Castelli and his colleagues, the presence/absence of a U-shaped spectrum is used as a "yes or no" indicator of significant proton acceleration in solar flare-bursts at the U. S. space forecasting centers in Boulder and Omaha.⁷⁻⁹ Moreover, the successful application of the U, coupled with the ability to view the sun through clouds at radio wavelengths, was a significant factor in the evolution of the worldwide solar radio patrol of the USAF¹⁰ and the establishment of the present day Radio Solar Telescope Network (RSTN)¹¹ that monitors solar emissions in the frequency range from 245 MHz to 15.4 GHz.

Despite the use of the U-shaped spectrum as a forecasting aid, however, certain questions about its development, pragmatic application, and physical interpretation remain unanswered. Kahler and Simnett (1980, private communications)

7. Heckman, G. (1979) Predictions of the space environment services center, in Solar Terrestrial Predictions Proceedings, vol. 1, p. 322, R. F. Donnelly, Ed., National Oceanic and Atmospheric Administration, Boulder, Colo.
8. Cliver, E. W., Secan, J. A., Beard, E. D., and Manley, J. A. (1978) Prediction of solar proton events at the Air Force Global Weather Central's space environmental forecasting facility, in Effect of the Ionosphere on Space and Terrestrial Systems, Conf. Proc., J. M. Goodman, Ed., U. S. Government Printing Office, Washington, D. C.
9. Thompson, R. L., and Secan, J. A. (1979) Geophysical forecasting at AFGWC, in Solar Terrestrial Predictions Proceedings, vol. 1, p. 350, R. F. Donnelly, Ed., National Oceanic and Atmospheric Administration, Boulder, Colo.
10. Castelli, J. P., Aarons, J., Guidice, D. A., and Straka, R. M. (1973) The solar radio patrol network of the USAF and its application, Proc. IEEE 61:1307.
11. Guidice, D. A., Cliver, E. W., Barron, W. R., and Kahler, S. (1981) The Air Force RSTN system, Bull. AAS 13:553.

pointed out that certain events in Castelli and Barron's list of 81 events did not appear to satisfy the stated definition of a U-burst, while other events whose peak-flux-density spectra conformed to the definition were omitted. A preliminary inspection of the data compiled in Solar Geophysical Data¹² and the Quarterly Bulletin of Solar Activity¹³ confirmed these apparent discrepancies and revealed others. Some of the difficulty lies in the definition of the U-shaped spectrum as stated by Castelli and Barron.⁵

The criteria . . . were that the flux density of the radio burst at time of maximum have a spectrum resembling a "U" where (1) flux density is rising in the short wavelength direction and is $\gtrsim 1000$ [sfu] in the $\lambda \sim 3$ cm range, (2) flux density in the decimeter range passes through an emission minimum, and (3) flux density in the long-meter-wavelength direction rises again to values $\gtrsim 1000$ [sfu].

A shortcoming of this definition is that it contains no mention of the allowable separation in time between peaks at different frequencies. For certain events in Castelli and Barron's (CB) list (Nos. 6, 17, 22, and 61), the low frequency maximum occurs from 10 to 50 min after the ~ 10 -GHz peak. In two of these events (Nos. 17 and 61), the ~ 200 -MHz emission did not begin until ≥ 15 min after the centimeter wavelength maximum. Constructing peak-flux-density spectra from discrete frequency peaks separated by tens of minutes strains the credibility of the U as a forecast tool (and as a meaningful physical construct), since, given enough time and the relative high frequency of bursts at the longer wavelengths, unrelated microwave and meter wavelength bursts might be combined to give U-shaped spectra. For other events on CB's list, the desired result, association of U-bursts with principal PCA events, was assumed. For the 02 December 1968 event (No. 25), observations were not available above 2700 MHz (Penticton, 270 sfu), but O'Brien, by applying the average spectral index in the 3- to 9-GHz range for radio bursts associated with principal PCAs deduced that the U-shaped criteria would have been satisfied for this event had observations been available at 9 GHz. For the 02 November 1969 event (No. 36) associated with a flare $\gtrsim 10^\circ$ behind the western limb, the highest flux value reported at frequencies < 1 GHz was 300 sfu (Moscow, 204 MHz). Castelli and Guidice¹⁴ make the assumption that had this event occurred on the visible disk, a high flux, presumably $\gtrsim 1000$ sfu, would have

-
12. Solar Geophysical Data, National Oceanic and Atmospheric Administration, Boulder, Colo.
 13. Quarterly Bulletin of Solar Activity, International Astronomical Union, Eidgen. Sternwarte, Zurich.
 14. Castelli, J. P., and Guidice, D. A. (1972b) The radio event associated with the polar cap absorption event of 2 November 1969, in Proc. of COSPAR Symposium on Particle Event of November 1969, p. 27, J. C. Ulwick, Ed., AFCRL-72-0474, AD 763081.

been recorded at the longer wavelengths, giving a U-shaped spectrum for this event in accordance with the stated criteria. There are other difficulties with the CB list. The U-burst on 24 May 1972 had low frequency emission \gtrsim 1000 sfu only at $f \sim 100$ MHz, but it is included in CB's list (No. 55) despite statements^{4,10} that the U-shaped signature for proton events applies only to the spectral range from 200 MHz to ~ 10 GHz. Finally, for the 01 November 1968 (No. 20) and 06 May 1969 (No. 34) events, the highest flux densities reported at $f \leq 1000$ MHz are 400 sfu and 325 sfu, respectively. While the appropriateness of the inclusion of the above-mentioned events on the U-burst list of Castelli and Barron is debatable, other events that satisfied the U-shaped spectral criteria were omitted from the list. Well-defined examples of such events occurred on 04 September 1966 (0417 UT), 04 March 1967 (1716 UT), 21 March 1969 (1334 UT), 14 January 1971 (1122 UT), and 06 March 1972 (1116 UT).

From our perspective, a more fundamental question than the classification of individual events in previous studies of U-shaped spectra and proton events concerns the basic methodology of these studies. Despite the considerable effort that has been expended on investigations of the U-burst/proton event relationship, no systematic study has been undertaken to classify the peak-flux-density spectra of large solar bursts into different types and then to compare the proton association of non-U types with that of the U-bursts. Thus at present, we know neither the approximate fraction of large radio bursts that have U-shaped spectra, nor the degree of association between large bursts with non-U spectra and proton events. Until these questions are addressed, it is difficult to assess the value of the U as a yes or no forecast tool since it is not known how well it discriminates against large microwave bursts of different spectral type.

Finally, questions about the physical interpretation of the U-shaped peak-flux-density spectrum have persisted since its introduction. In the original papers,^{1,2} little attempt was made to provide an explanation for the observed association between U-bursts and proton events. Subsequently, Castelli and Guidice⁴ interpreted this relationship in terms of a two-stage acceleration process. In their model, flash phase electrons accelerated downward toward the solar surface (or trapped on low-lying loops) give rise to the centimeter wavelength branch of the U. The intensity of the microwave peak (\gtrsim 1000 sfu in U-bursts) served as an indicator that the energy release during the impulsive phase was sufficient to produce a coronal shock wave (inferred from a Type II burst) through which the electrons accounting for the meter wavelength branch of the U and the protons observed at Earth were accelerated via a Fermi-type process. The idea of two phases of particle acceleration in flares was proposed by Wild et al¹⁵ and de Jager.¹⁶ The

References 15 and 16 will not be listed here. See References, page 50.

picture suggested by Castelli and Guidice for the relationship between the two stages is in qualitative agreement with the detailed model of Lin and Hudson.¹⁷ However, since Cliver et al^{18, 19} have shown that significant [$J(> 10 \text{ MeV}) \geq 10 \text{ pr cm}^{-2} \text{ sec}^{-1} \text{ sr}^{-1}$] proton events can be associated with relatively small [$\text{Sp} (\sim 9 \text{ GHz}) < 100 \text{ sfu}$] microwave bursts, as was also indicated by Castelli and Tarnstrom,⁶ the explanation of the U-burst/proton relationship proposed by Castelli and Guidice is problematical. Nevertheless, Lin²⁰ and Svestka and Fritzova-Svestkova²¹ have noted an association between Type II bursts and interplanetary proton events, and it would be interesting to see if large flare bursts with the U-shaped spectrum are preferentially associated with Type IIs in comparison with large non-U-bursts. Without such additional evidence for a physical link between U-bursts and proton events, the inclination is to dismiss the U-burst/proton event association as an example of the Big Flare Syndrome,²² perhaps useful for forecasting purposes but incapable of providing insights on the problem of proton acceleration in flares. In essence, the Big Flare Syndrome states that a flare that is prominent in one energy or wavelength tends to be prominent in all, and cautions about over-interpreting associations/correlations observed in samples of big flares.

In this study we classify the peak-flux-density spectra of all large radio bursts [$\text{Sp} (\geq 2 \text{ GHz}) \geq 800 \text{ sfu}$] observed from 1965 to 1979 and compare the associations of bursts of different spectral classes with interplanetary proton events and Type II/IV bursts. In addition, we examine the nature of the low frequency branch of the U-shaped spectrum and conduct a search for necessary conditions in the radio domain for the occurrence of a significant [$J(> 10 \text{ MeV}) \geq 10 \text{ pr cm}^{-2} \text{ sec}^{-1} \text{ sr}^{-1}$] proton event.

In the next section, we discuss our data sources, event selection criteria, and burst classification procedures and present the list of events to be analyzed. The various statistical associations are presented in the following section, and a summary and discussion of results are contained in the final section.

- 17. Lin, R. P. and Hudson, H. S. (1976) Non-thermal processes in large solar flares, Sol. Phys. 50:153.
- 18. Cliver, E. W., Kahler, S. W., Cane, H. V., Koomen, M. J., Michels, D. J., Howard, R. A., and Sheeley, Jr., N. R. (1983b) The GLE-associated flare of 21 August, 1979, Sol. Phys. 89:181.
- 19. Cliver, E. W., Kahler, S. W., and McIntosh, P. S. (1983c) Solar proton flares with weak impulsive phases, Astrophys. J. 264:699.
- 20. Lin, R. P. (1970) The emission and propagation of 40 keV solar flare electrons. I: the relationship of 40 keV electron to energetic proton and relativistic electron emission by the sun, Sol. Phys. 12:266.
- 21. Svestka, Z., and Fritzova-Svestkova, L. (1974) Type II radio bursts and particle acceleration, Sol. Phys. 36:417.
- 22. Kahler, S. W. (1982a) The role of the big flare syndrome in correlations of solar energetic proton fluxes and microwave burst parameters, J. Geophys. Res. 87:3439.

2. RADIO AND PROTON DATA (1965-1979)

By 1965, near the start of the 20th solar cycle, radio and particle patrols of the sun were reasonably complete. Radio coverage at a range of discrete frequencies was provided principally by patrols at Gorky (USSR), Berlin - Adlershof/Tremsdorf (DDR), Pennsylvania State University (USA), and Toyokawa/Hiraiso (Japan). [Sagamore Hill (USA) began reporting in January 1966.] Solar particle events in 1965 were monitored from space (e.g., IMP 2, IMP 3, PION 6) as well as by ground-based polar riometers.²³ The final year considered, 1979, was the last full year for which comprehensive radio, proton, and optical flare data were available at the time we began the study.

2.1 Radio Data Sources

For discrete frequency data we relied primarily on the Quarterly Bulletin of Solar Activity (QBSA) for events occurring before 1969 and Solar Geophysical Data (SGD) for subsequent years. Since the QBSA did not always list all peak-flux-density values/times when several stations reported observations at or near a given frequency, it was necessary to supplement this data source with the burst compilations from individual observatories such as Hiraiso, Toyokawa, Ondrejov, Gorky, and Slough. Also, for a few periods, data from certain observatories were not published in either QBSA or SGD and are only available in the individual observatory reports. The two prominent examples of this that we noted were for Manila (1968) and Toyokawa (1978). It is important to note that, for consistency, only tabulated data were used. Reference was not made to either published burst profiles or to the Sagamore Hill strip chart data which we have archived for the years 1966-1981.

2.2 Selection Criteria

In our search for large microwave bursts occurring during this period, we used the following selection criteria:

- (a) $Sp \geq 800$ sfu at $f \geq 2$ GHz, and
- (b) $85^\circ E \geq \phi \leq 85^\circ W$,

where SP = peak radio flux density, and ϕ is the longitude of the associated H α flare. We considered frequencies ≥ 2 GHz since this frequency serves as a nominal divider between the decimetric wavelengths, where intense narrow band features often occur without significant associated microwave emission, and the

23. Bailey, D. K. (1964) Polar cap absorption, Planet. Space Sci. 12:495.

centimetric wavelengths, where spectral variations are typically smoother.²⁴ The ≥ 800 -sfu level is roughly equivalent to Castelli and Barron's $\gtrsim 1000$ -sfu level. In our initial screening of the data we selected all events for which any observatory reported a peak flux value ≥ 800 sfu at any frequency ≥ 2 GHz. We then eliminated those events for which reported flux values ≥ 800 sfu were not supported by observations at the same or adjacent frequencies, when such observations were available. The solar longitude criterion was adopted to screen out events occurring close to or beyond the limb for which the radio source may have been partially occulted. The 193 events satisfying these selection criteria are listed in Table 1. Event date, ~ 10 -GHz maximum time, ~ 200 -MHz maximum time, and H α flare location and classification are given in columns two through six, respectively. The time of the 10-GHz maximum (200-MHz maximum) was obtained by averaging the reported times at frequencies from 8.2 to 11.8 GHz (184 to 328 MHz). For event Nos. 14, 21, 30, 75, 76, 163, and 170, H α flare associations are questionable since two candidate optical events were in progress at the time of the radio burst. The listed flare is, in our opinion, the more likely source of the intense microwave emission.

2.3 Constructing Spectra

Several of the events in Table 1 had more than one reported peak in their flux-density time profiles that satisfied our Sp (≥ 2 GHz) ≥ 800 sfu selection criterion (e.g., two of the large bursts in the August 1972 sequence, Nos. 98 and 101). For such events, we constructed spectra at the time of the largest peak at the highest frequency for which observations were reported. Since secondary (late) peaks in microwave outbursts tend to have their maxima at progressively lower frequencies,^{25,26} this procedure was designed to select the initial major peak in the listed events. While this tactic did not always, in fact, identify the first reported centimeter wavelength peak ≥ 800 sfu (e.g., Nos. 16 and 98), it did ensure a consistent approach to the data. We considered only those lower frequency flux-density maxima that fell within a five-minute sliding window containing the highest frequency/highest flux "anchor time". No two discrete frequency maxima that were used to determine the peak-flux-density spectrum could be separated in time by more than five minutes. The five-minute

-
- 24. Kundu, M. R. (1965) Solar Radio Astronomy, Interscience Publishers, New York, New York.
 - 25. Kai, K. (1968) Evolutional features of solar microwave type IV bursts, Pub. Astron. Soc. Japan 20:140.
 - 26. Kahler, S. W. (1982b) Radio burst characteristics of solar proton flares, Astrophys. J. 261:710.

Table 1. Large Microwave Bursts 1965-1979: Peak-Flux-Density Spectra, and Sweep Frequency Burst and Proton Association

DATE <u>T21</u>	MAX <u>T41</u>	200 MHZ MAX	SOLAR TIME†	Hα COORDS <u>T51</u>	200 MHz FLUX <u>T71</u>	500 MHz FLUX <u>T71</u>	1 GHz FLUX <u>T81</u>	3 GHz FLUX <u>T81</u>	10 GHz FLUX <u>T101</u>	FREQ OF AT <u>T111</u>	HIGH FLUX AT <u>T121</u>	FREQ OF AT <u>T131</u>	HIGH FLUX AT <u>T141</u>	TYPE PR <u>T151</u>	TYPE INT <u>T161</u>	TYPE INT <u>T171</u>	>10MeV <u>T181</u>		
1 651002 0414.6	0415.0	N22E12	2	-3	-3	120	350	900	1000	120	9500	850	2	N.O.	N.O.	-	-		
2 660117 1111.0	(1143.5)	N19E27	28	-5	-5	950	420	960	1000	160	9500	440	2	N.O.	N.O.	-2	-		
3 660319 0343.7	-	N21E34	3N	-1	880	350	710	4200	1000	350	9500	3600	1	-	-	-	-		
4 660320 0956.4	(1035.0)	N20E18	28	-5	130	540	1750	2300	1500	390	9500	2300*	1	N.O.	N.O.	-2	-		
5 660324 0231.7	(0234.5)	N20W42	2N	2000	560	160	440	960	1000	440	6000	2600	9500	2200	1 1233(k)	Xk	-		
6 660330 1249.9	1253.8?	N28E50	2N	24000	600	450	1800	2100	800	430	950012500	17000	8000	1	0038	X	-	1	
7 660707 0037.5	0038.6	N35W48	28	900	900	1400	3200	12500	400	320	8000	3500	11000	3300	1	1531	X	1	
8 660828 1526.9	1527.4	N22E04	2+	70000	-3	1600	1000	3300	2100	320	17000	10000	1	0554.5	-	-	2		
9 660902 0555.8	0556.0	N22W58	3+	3300	-3	1400	2300	7000	1000	1400	17000	10000	1	0554.5	-	-	2(M)		
10 660918 1456.4	(1508.5)	N22E42	18	-5	300	330	820	1000	11000	930	7 1459.8	-	-	X	-	-	-2(M)		
11 670227 1649.3	1645.7?	N27E02	2+	2000	700	600	840	5000	2000	600	10000	5000	1	1640	Xk	Xs	0		
12 670304 1716.2	N.O.	N24W68	1B	-	-212000	48	500	1150	1000	48	10000	1150	1	1718	-	-	-2(M)		
13 670322 0032.0	-	N24E68	3-	-1	-5	250	1200	2000	7500	2100	17000	1650	3	-	X	-	-		
14 670520 1520.4	1515.4	N23E51	1B	-5	180	280	700	560	5500	1350	11000	500	2	1520	Xk	Xs	-		
15 670521 1925.5	1923.7	N24E39	2N	1100	2100	1000	960	1700	1500	720	7000	2100	11000	1400	1	1923	Xs	-2	
16 670523 1947.0	N.O.	N27E28	2B	-	-219200	-5	6800	27000	2700	6400	900023000	1	4838	X	X	1			
17 670528 0542.0	0540.5	N28W33	3B	3000	600	1000	1100	7800	600	500	12000	8800	17000	5000	1	0539	-	2	
18 670725 1427.6	-	N28E39	1B	-1	6	40	235	1400	110	45	9000	1200	3	-	-	-	-		
19 670829 1330.9	1331.7	N23W44	2B	1050	240	70	110	950	1700	45	9000	840	1	-	Xs	-	-		
20 680111 1700.8	1703.4	S25W39	1B	-3	150	-5	280	1400	1400	9000	1500	15000	630	7 1703	Xk	X	-1		
21 680201 1803.0	1803.0	S15E48	SN	-5	235	180	170	380	2300	160	15000	840	7 1820	-	Xs	-2(A)			
22 680503 2130.0	2128.2	N19E49	1B	150	100	90	135	1000	2700	1200	12500	1200	15000	1100*	2 2127.8	Xs	-2		
23 680609 0850.8	0847.8	S14W08	3B	3000	-5	570	1000	1200	1200	560	5000	1600	19000	360	-	Xc	X	2	
24 680708 1711.6	1710.9	N13E59	3B	>105	3500	1200	1600	5000	1600	800	15000	5600	19000	5600	1	1708.8	X	0	
25 680808 1816.6	-	N10W01	2B	-1	11	57	475	1900	520	520	15000	2400	3	-	-	-	-2(M)		
26 680926 0030.2	0030.0	N14E35	2B	230	-2	580	340	960	3000	340	9500	930*	1	0034.5	-	Xs	0		
27 680929 1620.1	1619.5	N17W52	2B	8500	370	220	730	2300	750	190	9000	2400	19000	660	1 1619	Xs	1		
28 681021 0605.6	-	N17E29	2B	-1	-1	180	1250	-1	180	1250	9500	1250*	3	-	X	-	-		
29 681027 1235.5	-	S17E16	1B	-4	3	50	750	1650	5500	2000	15000	1400	3	-	X	-1	-		
30 681029 1522.1	1525.0	S14W19	1N	5000	>105	90000	4000	520	520	>105	19000	220	7	-	X	-	0(A)		
31 681031 0011.1	0009.0	S14W37	3B	790	5000	470	1800	1800	1000	470	5000	2800	17000	940	1 2359	X	2		
32 681031 2251.4	2255.5	S14W49	2B	1400	-5	190	-5	2050	1000	190	8000	2200	9500	2100	-	Xs	1(M)		
33 681101 0912.4	(0846.5)	S18W47	1B	-5	190	560	2000	1800	1800	2700	2500	380	15000	4000	1	0851.7	Xc	-2	
34 681104 2004.6	2004.7	S13W57	1B	6600	2500	1000	420	750	1650	5500	2800	19000	1000	2	2007	-	Xs	1(N)	
35 681102 0956.0	0953.0?	S15W65	2B	550	-3	-2	700	7500	12000	8000	19000	6300	7 1003.5	Xc	X	1(M)			
36 681227 1056.0	1057.5	N16E02	2B	2800	350	320	800	3000	650	230	12000	3100	70000	1200	1	1055.5	Xk	Xs	-1
37 690117 1704.5	1703.0	N17E46	SB	-5	640	230	520	1400	900	230	25000	2400	35000	2200*	1	1705.6	X	-1(A)	
38 690220 0619.4	-	N15E38	2B	-1	10	28	400	820	820	9000	850	17000	500	3	-	-	-	-	

Table 1. Large Microwave Bursts 1965-1979: Peak-Flux-Density Spectra, and Sweep Frequency Burst and Proton Association (Contd)

DATE	TIME ₁	TIME ₂	MAX	200 MHz MAX	200 MHz TIME ₁	200 MHz TIME ₂	SOLAR WINDS	H _a CL	200 MHz FLUX	500 MHz FLUX	1 GHz FLUX	3 GHz FLUX	10 GHz FLUX	FREQ OF AT	HIGH FLUX	TYPE	>10 MeV				
																11	SP	11	TYPE	PR	INT
39	690224	2314.1	2314.0	N12W32	28	640	850	300	620	860	1400	220	6000	1200	9000	940	1	2311.5	x	x	-1
40	690225	0912.6	0912.4	N13W37	28	50000	13000	6000	2250	5800	2800	2200	10000	5800	19000	4700	1	-	x	x	1
41	690226	0425.3	0425.5	N13W46	28	-3	7000	1200	1100	3500	1500	550	10000	3500	17000	3000	1	0425.5	-	xs	1
42	690227	1408.4	1407.6	N13W65	28	3600	1300	500	900	2700	1400	410	8500	2900	19000	1850	1	1404.4	x	xs	1
43	690312	1741.0	1741.8	N12W80	28	2500	415	700	1650	4000	470	410	17000	5000	35000	2700	1	1740.8	x	x	0
44	690321	0150.0	0149.0	N19E16	2N	380	-5	290	800	1000	6000	2000	6000	2000	9500	1100	2	0150	-	xs	0
45	690321	1333.6	1334.8	N19E09	2B	-5	2000	2350	1800	7000	2700	1600	9000	7100	35000	4700	1	1334	x	xs	0(M)
46	690321	1944.3	1944.9	N21E06	1B	500	13	-1	25	1000	600	6	11000	1000	15000	880	2	-	-	xs	0(M)
47	690327	1330.2	1328.3	N20W70	2B	600	35	92	860	3800	500	35	20000	6000	4800	2	1331	x	xs	-1	
48	690329	1922.9	-	N10E54	1B	-1	-1	5	130	1000	11000	1050	15000	700	3	-	-	-	-	-2(M)	
49	690421	2008.8	2007.8	N24W32	3B	950	180	340	1350	3500	600	160	8500	3600	35000	2200	1	-	x	xs	0(M)
50	690426	2307.5	2307.0	N08E38	2N	1500	330	270	450	600	750	250	5500	880	15000	640	1	2305.2	x	xs	-1(M)
51	690506	0243.0	(0249.0)	S31E67	1B	-5	220	320	210	1350	1800	160	9500	1300	7	N.O.	N.O.	N.O.	-2(M)		
52	690505	1001.4	0959.3	N12E63	3B	4000	520	400	-5	4700	900	390	12000	4800	70000	2300	1	0957	x	xs	-2
53	691118	1650.6	1651.0	N14E40	2B	6000	1400	370	-5	5400	1500	260	8000	6000	35000	2100	1	1648	x	x	-2
54	691119	0537.1	0539.5	N14E53	1B	25	70	420	1500	1300	4000	1700	9000	1350	3	-	-	-	-	-2(M)	
55	691120	1621.1	-	N07E08	2B	-1	-1	6	460	800	7000	1150	35000	160	3	-	-	-	-	-2(M)	
56	691123	1017.2	-	N15W19	1B	-1	80	450	280	1400	3000	280	12000	1450	19000	1050	3	N.O.	N.O.	N.O.	-2(M)
57	691124	0918.8	0920.5	N15W31	2B	18000	700	1000	2600	1000	820	220	3000	2600	70000	1600	1	N.O.	N.O.	N.O.	0
58	691127	1932.4	1933.5	N18W83	2B	11000	6200	1500	950	3600	1750	700	5000	2600	35000	860	3	-	-	-	-1(M)
59	700128	1919.7	-	S14W33	2B	-1	2	35	1200	1500	4000	1700	9000	1350	3	-	-	-	-	-1(M)	
60	700211	0706.9	0710.7	N18W06	2B	120	13	95	2100	4100	620	10	6000	5200	35000	1000	2	0710	-	-	-2
61	700301	0938.5	0938.4	N05E48	1B	17000	3400	1350	800	1300	2500	780	10000	1300	35000	640	1	0936.5	xc	xs	-
62	700301	1127.7	1128.1	N13W31	2B	8000	-5	-5	470	740	3000	470	5000	1450	19000	390	1	1129	-	xs	-
63	700301	1530.8	1530.4	N05E46	1B	3000	3400	1200	540	680	2500	500	5500	840	35000	800	1	1531.5	x	xs	-
64	700329	0040.8	(0102.4)	N13W37	2B	-5	-5	7600	1300	5100	2200	1000	7500	5400	17000	3800	1	0040	x	x	1
65	700326	1122.6	-	S07E18	-B	-1	-1	-1	3	1900	920	1000	9000	1050	70000	175	3	-	-	-	-
66	700613	0659.0	0702.7	N20L23	1B	2200	1100	220	220	960	1700	130	12000	980	19000	800	1	-	-	xs	-
67	700613	0922.3	0925.2	N18E53	1B	110	500	45	220	840	1200	420	10000	9200	70000	2200	1	0925	-	xs	-
68	700614	0507.4	0510.7	N19E42	2B	20	15	95	680	1150	400	13	7000	1250	9500	1180	3	0512.5	-	-	-
69	700614	1325.8	1324.9	N21E42	2B	1500	2300	4500	700	3000	2200	540	7500	3200	70000	1500	1	1324.6	x	xs	-1(A)
70	700614	1703.9	-	N19E35	1B	-1	35	8	600	920	1000	8	35000	960	3	-	-	-	-	-1(A)	
71	700628	2002.9	2001.2	N20L23	1B	1050	530	500	420	760	2800	410	8000	840	15000	450*	1	2007.5	x	xs	-2
72	700720	1123.0	1122.9	N08E55	2B	1500	660	440	2000	920	420	10000	9200	70000	2200	1	-	-	xs	-	-
73	700722	0030.5	0030.0	N09E32	2B	370	1900	1050	1350	4800	1400	470	5500	7400	17000	3100	1	-	-	xs	-1(M)
74	700723	1845.1	1846.0	N09E09	1B	-3	7000	-5	1100	3800	2800	1050	11000	4000	35000	1900	1	-	-	xs	1
75	700814	1614.7	1618.8	N11E74	1B	2000	65	70	-5	450	700	54	5000	960	35000	240	1	-	-	xs	1(A)
76	701028	1252.3	1251.6	N21E20	2B	9000	1000	1600	620	2000	2800	580	12000	2050	35000	11000*	1	1254	x	xs	-2
77	701105	0326.7	(0339.0)	S12E36	3B	-5	-5	290	880	1100	6000	1700	9000	1200	6000	12000	7	0324	x	x	-1

Table 1. Large Microwave Bursts 1965-1979: Peak-Flux-Density Spectra, and Sweep Frequency Burst and Proton Association (Contd)

DATE (2)	TIME (3)	MAX FLUX (4)	TIMEIT (5)	SOLAR WAVE INDEX (6)	H _a FLUX (7)	NHZ FLUX (8)	GHZ FLUX (9)	GHZ FLUX (10)	200	500	1	3	10	FREQ FLUX	HIGH FLUX	TYPE	>10MEV				
									MAX	MIN	AT	AT	FREQ	AT	SP	TYPE	PR				
									MAX	MAX	MAX	MAX	MAX	MAX	INT	INT					
78 701115	0753.5	-	N16W11	1N	-1	100	140	690	1100	1400	100	6000	1250	9000	1330	3	-1				
79 701116	0050.8	-	N16W21	2B	-1	-4	180	2900	6800	8000	7200	9500	7000	3	0112	x	-1				
80 701117	0735.4	-	N16W38	2B	-1	-4	350	1400	1000	300	10000	1400	3	-	-	-2(M)					
81 701211	1028.4	1030.8	N10E36	1B	>105	1000	300	550	180	2400	1200	35000	2100	1	1030	x	-				
82 701211	2318.0	2315.5	N16W02	1N	350	-5	700	900	1100	1000	155	10000	1100	35000	220	2	2238	x	0		
83 710114	1122.2	1122.0	S09W56	1B	3700	400	155	310	7400	1400	640	7500	9200	9000	8100*	1	2315.6	x	-2		
84 710116	(0936)	(0926.8)	N19E66	2N	-5	2500	-5	2200	-5	3000	2200	7	-	-	-	-	-2(M)				
85 710124	2322.8	2320.0	S18W49	3B	800	640	800	2750	1200	1500	310	5000	3300	35000	450*	1	N.U.	N.O.	1		
86 710406	0943.9	0941.0	S19W80	-B	-4	3000	960	1200	1500	8000	1300	9000	1280	2	-	xc	-	-			
87 710420	0518.6	0520.0	N20W20	2B	200	4	28	370	1200	580	3	35000	1150	2	1518.4	x	x	-1(A)			
88 711122	1519.4	(1526.7)	N15E72	1B	-5	-5	-5	2800	100	1050	100	9000	120	7	0549	-	x	-1(A)			
89 711123	0553.8	(0559.5)	S19E60	1B	-5	50	-5	1050	160	5000	1300	10000	680	1	-	x	-	-2			
90 720213	0830.2	0830.9	S18E47	1B	2100	165	290	1050	680	540	2400	450	2	-	x	x	-				
91 720216	(1740.2)	(1801.0)	N24E04	-N	-5	-5	-5	850	-4	2800	2800	850	7	-	x	x	-				
92 720222	0032.7	0032.6	N03W02	2N	1600	520	850	1200	940	500	2500	1300	1700	570	1	0036	x	x	-1		
93 720305	0815.0	0815.7	S07E43	1B	45000	3800	1100	2100	4400	950	1100	11000	4500	35000	1800	1	N.O.	N.O.	0(A)		
94 720306	1116.2	1118.6	S08E26	1B	13000	1700	470	500	1800	1700	320	12000	1900	35000	1400	1	1117.7	x	x	0(N)	
95 720524	0701.8	0704.0	S08E85	1N	340	50	200	630	2400	450	32	19000	8000	2	0703.1	x	x	-			
96 720528	1327.2	(1400.0)	N09E30	2B	-5	-5	1900	1500	5600	1400	1050	9000	5700	35000	1800	1	1327.5	x	x	-	
97 720603	1409.0	1408.8	N09W53	1N	3000	50	-4	4000	16000	2700	3900	18000	24000	35000	13000	1	1451	x	x	-2	
98 720802	0404.1	(0339.5)	N12E34	3N	-5	580	2200	2100	5000	2600	9500	2200	?	-	-	-	-	0			
99 720802	1839.8	-	N14E26	1B	-1	17	60	720	480	5000	900	35000	840	3	-	xc	-	0(N)			
100 720802	2144.8	2143.6	S14E28	2B	5500	>105	-5	9500	6700	10000	4500	40000	100000	35000	950	1	-	0(M)			
101 720804	0627.1	0625.0	N14E08	3B	-3	-5700000	-5	18000	20000	5400	19000	25000	70000	12000	1	-	x	x	4		
102 720807	1523.7	1524.6	N14W37	3B	1200	9000	-3	4000	16000	2700	3900	18000	24000	35000	13000	1	1518.8	x	x	3	
103 721026	0647.2	-	S12E47	1B	-1	-1	-1	60	1100	165	1000	1200	13000	3000	1200	9000	1050	3	-	-	-
104 721030	0729.1	(0744.7)	S10W03	1B	-4	50	110	165	1250	1400	120	950	2600	52	10000	1000	3	N.U.	N.O.	1(A)	
105 721216	0347.5	0347.5	N12W57	1B	240	170	840	275	1250	1400	120	900	1200	1	0343	x	x	-1			
106 730111	0049.4	0048.0	N11W80	1B	330	60	170	56	950	2600	52	950	900	2	0047	x	x	-2			
107 730301	1119.6	1120.7	N08W07	1B	800	270	2200	470	1400	2700	440	9500	1450	70000	220	1	1120.1	-	x	-	
108 730429	2102.9	(2215.3)	N14W73	2B	-5	2000	3000	1200	13000	3000	1200	35000	39000	1	2101	x	x	1			
109 730503	0833.3	0836.0	S14E51	2B	40000	540	380	1100	2000	1000	380	70000	21000	1	0834.5	x	x	-2(M)			
110 730517	1908.6	1908.3	N08E53	1B	2000	48	21	68	900	800	19	13000	950	35000	420	1	1911	-	x	-2(M)	
111 730518	2156.4	2156.6	N10E33	-B	1200	600	140	70	390	2300	60	35000	800	1	-	x	-	-2(M)			
112 730519	2244.5	2243.1	N09E19	2B	1500	320	210	1400	920	650	220	2700	1700	15000	600*	1	2248.8	-	x	-2(M)	
113 740602	0426.2	0426.87	S13E48	1N	-5	1400	260	380	1500	1800	180	9500	1400	1	-	-	x	-			
114 740630	2229.0	2228.0	S12E45	-B	1500	270	140	450	880	900	130	8000	1000	3500	1	-	x	-	-2(A)		
115 740702	0715.9	0715.2	S14E23	1N	30000	5500	440	370	780	2000	240	5000	1400	700	700	1	840	-	x	-2(A)	
116 740703	0836.4	0833.8	S14E08	2B	30000	27000	4100	1000	4100	1600	9500	38000	1	-	x	x	-1(M)				

Table 1. Large Microwave Bursts 1965-1979: Peak-Flux-Density Spectra, and Sweep Frequency Burst and Proton Association (Contd)

DATE [2]	TIME [3]	10 GHz		200 GHz		500		1		3		10 GHz		FLUX		FREQ		FLUX		HIGH FLUX		TYPE		>10 MeV																		
		MAX	MAX	SOLAR	Hα	MHz	MHz	GHZ	GHZ	FLUX	FLUX	FLUX	FLUX	FLUX	FLUX	AT	OF	AT	SP	II	TYPE	TYPE	PR	INT	III	IV	V	ONSET	T167	T177	T187	T197	T207	T217	T227							
117	740704	0648.5	S14W05	1B	14000	9600	3500	1500	-1	-1	5	4700	2200	960	9500	4400	1	-	X	X	1(h)																					
118	740704	1115.1	S15W06	-B	100	-1	-1	-1	5	1600	3700	5000	330	1600	3000	330	10000	1600	35000	900	-	X	O(M)																			
119	740704	1354.6	S15N08	2B	-3	-3	-5	1600	3500	330	1600	3000	430	1650	550	180	22000	2300	35000	1150	1	-	X	X	1(M)																	
120	740704	2058.8	(2109.8)	S16W12	IN	-5	5000	3500	330	1600	3000	400	1350	1800	4000	10000	1350	12000	4100	35000	1800*	1	-	X	X	2(M)																
121	740705	1511.0	S15N23	1B	1100	180	400	430	1650	550	180	20000	4000	1350	1800	4000	10000	1350	12000	4100	35000	1800*	1	-	X	X	2(M)															
122	740705	2139.5	2142.7	S15W26	1B	20000	4000	1350	1800	4000	10000	220	1400	80	1000	540	76	20000	1700	70000	540	2	-	X	X	1(h)																
123	740706	1037.1	1036.6	S15W31	-B	400	80	220	240	1000	1000	560	140	35000	1200	70000	660	1	-	X	X	1(h)																				
124	740706	1111.5	1110.9	S16A35	1B	30000	220	350	800	560	560	140	35000	1200	70000	660	1	-	X	X	1(h)																					
125	740706	1904.7	1903.6	S16A39	1B	300	1000	250	360	1400	1400	130	35000	1750	1	-	X	X	1(M)																							
126	740910	2140.6	2143.4	N10E51	2B	2500	9500	1500	-3	9500	10000	1500	10000	9500	35000	4000	1	2136.2	X	X	1																					
127	740919	2239.5	2238.5	N09A62	2N	-3	760	1320	2200	2900	1700	620	7000	3300	9500	3000	1	2232.8	X	X	1																					
128	741011	0329.3	0331.5?	N12E02	1N	-3	350	370	460	1900	1000	370	9000	1700*	7	0335(k)	X	X	-1																							
129	741011	1446.3	1446.6	N12A03	1B	800	160	620	450	1400	1400	200	8000	1600	35000	220*	1	-	X	X	-2(M)																					
130	741015	1325.6	-	N08A47	1B	-1	22	250	280	820	1500	72	8000	900	15000	640	3	-	-	-	-																					
131	741105	1535.4	1535.2	S12W78	IN	1100	2300	380	94	380	2800	94	35000	2100	1	1536.5	X	X	1																							
132	750811	1520.0	1520.8	S12W74	1B	5000	1100	270	160	1450	1700	120	35000	2200	1	1519.8	X	X	0																							
133	760328	1934.2	(1932.4)	S07E28	1B	-5	2500	1200	2200	3400	1500	540	8000	3500	35000	980	1	1921	X	X	-1																					
134	760430	2108.2	2107.5	S08A46	1B	600	3000	2900	1750	3000	2800	1700	11000	3100	35000	1200	1	2106.2	X	X	2																					
135	770909	1634.8	1633.8	N08E84	1N	120	70	230	-5	5500	500	70	15000	6200	35000	3600	2	1638	X	X	0(M)																					
136	770916	2308.0	(2245.4)	N07H20	2N	-5	2300	-3	1500	620	2200	3000	400	15000	10000	35000	80	7	2233.2	X	X	-1																				
137	770919	1036.6	1040.3	N08A57	3B	170	-2	1000	400	2200	3000	400	15000	10000	35000	2450	1	1038.5	X	X	2																					
138	771012	0151.4	0151.6	N06N02	1B	3800	6600	1700	500	1500	2000	440	10000	1500	35000	400	1	0153	X	X	0																					
139	771122	1003.3	1005.9	N24A40	2B	850	350	470	1450	4000	540	340	9500	3900	1	-	X	X	-2																							
140	780107	0638.2	0636.0	S16A65	1F	200	110	115	1300	2100	700	90	7000	2300	35000	950	2	-	-	-	-	-																				
141	780108	0714.2	0711.8	S12A85	2B	600	160	76	65	1300	2200	58	9000	1100	2000	740	1	1320.5	X	X	-1																					
142	780211	1427.3	1427.4	N14E06	1B	4500	850	400	115	360	2800	105	6000	400	15000	850	1	1908	X	X	2(M)																					
143	780410	1055.5	1057.3	N20T75	1B	3200	5000	1700	200	800	1450	75	10000	800	35000	230	1	1055.3	X	X	-2(M)																					
144	780411	1354.3	1354.2	N22N56	3B	50	1250	400	350	720	1500	200	20000	900	35000	820	1	1358.8	X	X	1																					
145	780425	1541.6	-	N18E72	1B	-1	500	30	2500	32	1000	30	2700	5600	9000	30*	3	-	-	-	-	-																				
146	780428	1329.0	1332.5	N22E38	3B	3000	10000	26000	-3	7200	5000	4000	10000	7200	35000	740	1	1320.5	X	X	2																					
147	780429	1914.5	1913.8	N20E14	2B	8000	5000	2000	1450	4400	2000	1300	9000	4500	35000	1100	1	1908	X	X	2(M)																					
148	780430	1446.2	1443.3	N28E14	3B	600	-5	1000	1400	1600	7000	2200	35000	1500	15000	350	1	1943	X	X	2(M)																					
149	780501	1953.5	(1947.0)	N21W12	2B	-5	-5	-5	-5	960	3200	1000	250	9000	3400	35000	740	1	1943	X	X	2(M)																				
150	780507	0329.7	0330.4	N23W72	1N	11000	1200	250	880	3200	1000	250	9000	3400	35000	870	1	0327.5	X	X	2																					
151	780508	1231.8	(1222.6)	N22W16	1B	-5	110	105	90	1600	54	12000	920	15000	740	1	1213.4	X	X	0(M)																						
152	780626	1541.3?	1537.8	N17W15	2B	350	380	270	1600	170	950	260	2800	1700	11000	150	2	-	X	X	-1(M)																					
153	780709	1828.2	(1834.0)	N19W68	2B	-5	500	-5	480	1800	1600	1400	1700	10000	40	5500	2700	35000	70	1	0428.4	X	X	-2(A)																		
154	780710	0642.9	(0648.0)	N18E51	3B	-5	160	1400	1700	10000	50	110	1800	1500	600	40	5500	2700	35000	70	1	0428.4	X	X	0(A)																	
155	780711	0427.9	0429.2	N12E81	1N	1500	50	110	1800	1500	600	40	5500	2700	35000	70	1	0428.4	X	X	0(A)																					

Table 1. Large Micromagnetic Fluctuations: Peak-Flux-Density Spectra, and Sweep Frequency Burst and Proton Association (Cont'd.)

DATE	10 GHz MAX	200 GHz MAX	10 GHz FLUX MAX	200 GHz FLUX MAX	TYPE		PR		>10 MeV		
					PERIOD	PERIOD	PERIOD	PERIOD	PERIOD	PERIOD	
15.6 780711	1543.3	-	1543.3	-	45.1	35.0	22	15.000	11.000	35000	890
15.6 780711	1052.3	1052.3	1052.3	-	45.1	15.0	29.0	15.000	10.000	35000	1051.3
15.8 780711	2350.7	-	-	-	45.1	1.0	1.0	220.0	29.0	35000	2350*
15.9 780712	1605.7	1605.7	1605.7	-	45.1	1.0	1.0	100.0	6.0	600	1
16.0 780715	1423.7	1601.1	1601.1	-	45.1	1.0	1.0	100.0	1.0	1	-
16.1 780711	2134.7	-	-	-	45.1	1.0	1.0	250.0	10.0	35000	930
16.2 780718	0.0	1801.7	1801.7	-	45.1	1.0	1.0	250.0	10.0	35000	17
16.3 781211	(2012.9)	2614.7	2614.7	-	45.1	1.0	1.0	280.0	14.0	1500	1
16.4 781212	2354.7	-	-	-	45.1	1.0	1.0	280.0	19.0	35000	1690
16.5 781214	0.0	1723.7	1723.7	-	45.1	1.0	1.0	280.0	11.0	15000	929
16.6 790103	0.0	2020.7	2020.7	-	45.1	1.0	1.0	300.0	10.0	9000	950
16.7 790205	0.0	2040.7	2040.7	-	45.1	1.0	1.0	300.0	10.0	35000	58
16.8 790205	2141.7	1801.7	1801.7	-	45.1	1.0	1.0	350.0	10.0	4100	1213.5
16.9 790216	0.0	1615.7	1615.7	-	45.1	1.0	1.0	350.0	10.0	850	1.045.5
17.0 790218	1641.7	1641.7	1641.7	-	45.1	1.0	1.0	350.0	10.0	1500	0.0
17.1 790309	1029.7	1029.7	1029.7	-	45.1	1.0	1.0	350.0	10.0	9000	350*
17.2 790403	0.0	1401.7	1401.7	-	45.1	1.0	1.0	350.0	10.0	600	1.027
17.3 790427	0.0	1646.7	1646.7	-	45.1	1.0	1.0	350.0	10.0	1700	3910
17.4 790603	1430.7	1430.7	1430.7	-	45.1	1.0	1.0	350.0	10.0	1000*	1
17.5 790605	0.0	1533.7	1533.7	-	45.1	1.0	1.0	400.0	37.0	35000	1150
17.6 790814	1246.7	1246.7	1246.7	-	45.1	1.0	1.0	400.0	37.0	35000	0.514
17.7 790820	924.5	924.5	924.5	-	45.1	1.0	1.0	400.0	37.0	35000	-
17.8 790820	1646.7	1646.7	1646.7	-	45.1	1.0	1.0	400.0	37.0	35000	-
17.9 790914	0.0	1737.7	1737.7	-	45.1	1.0	1.0	400.0	37.0	35000	-
18.0 790916	937.7	-	-	-	45.1	1.0	1.0	400.0	37.0	35000	-
18.1 790919	2309.7	-	-	-	45.1	1.0	1.0	400.0	37.0	35000	-
18.2 790921	2352.5	-	-	-	45.1	1.0	1.0	400.0	37.0	35000	-
18.3 791019	0.0	0.0	0.0	-	45.1	1.0	1.0	400.0	37.0	35000	-
18.4 791019	1151.7	-	-	-	45.1	1.0	1.0	400.0	37.0	35000	-
18.5 791105	2347.4	2347.4	2347.4	-	45.1	1.0	1.0	400.0	37.0	35000	2347
18.6 791106	0.0	0.0	0.0	-	45.1	1.0	1.0	400.0	37.0	35000	-
18.7 791119	2151.2	1616.7	1616.7	-	45.1	1.0	1.0	400.0	37.0	35000	-
18.8 791119	2131.7	1124.7	1124.7	-	45.1	1.0	1.0	400.0	37.0	35000	-
18.9 791119	0.0	0.0	0.0	-	45.1	1.0	1.0	400.0	37.0	35000	-
19.0 791119	0.0	0.0	0.0	-	45.1	1.0	1.0	400.0	37.0	35000	0.0
19.1 791119	2131.7	1124.7	1124.7	-	45.1	1.0	1.0	400.0	37.0	35000	-
19.2 791220	0.0	0.0	0.0	-	45.1	1.0	1.0	400.0	37.0	35000	-
19.3 791220	0.0	0.0	0.0	-	45.1	1.0	1.0	400.0	37.0	35000	0.0

Table 1. Large Microwave Bursts 1965-1979: Peak-Flux-Density Spectra, and Sweep Frequency Burst and Proton Association (Contd)

Notes:

† Notation used in this column is as follows: "?" ≡ time uncertain, and "()" ≡ the listed time is for the 3 GHz maximum.

†† Notation used in this column is as follows: "?" ≡ time listed as uncertain in SGD or QBSA, or time inferred from time of maximum at an adjacent frequency; "-" ≡ a station was observing at this frequency but did not report an event; "N.O." ≡ no observatory was on patrol at 200 MHz; and "()" ≡ the listed time occurred outside the sliding five-minute window.

* The following events require additional frequency - peak-flux-density pairs to describe their spectrum in the 200 MHz to 10 GHz range: No. 4 (1.5 GHz, 920 sfu), No. 22 (1.4 GHz, 640 sfu), No. 26 (2.0 GHz, 1200 sfu), No. 28 (1.4 GHz, 3 sfu), No. 37 (400 MHz, 1100 sfu), No. 67 (400 MHz, 800 sfu), No. 71 (1.4 GHz, 3200 sfu), No. 76 (1.4 GHz, 2400 sfu), No. 85 (600 MHz, 1300 sfu), No. 86 (650 MHz, 17 sfu), No. 112 (5.0 GHz, 620 sfu), No. 122 (1.4 GHz, 3300 sfu), No. 128 (600 MHz, 560 sfu), No. 129 (400 MHz, 2600 sfu), No. 145 (5.0 GHz, 25 sfu), No. 158 (1.4 GHz, 76 sfu), No. 171 (650 MHz, 1150 sfu), No. 174 (1.4 GHz, 1600 sfu), and No. 176 (400 MHz, 1300 sfu).

width of the time window was arbitrarily chosen, and, while it may still be too large to provide physically meaningful spectra, it is an improvement on the relatively open-ended approach of Castelli and Barron.⁵ In practice, as we shall show, large microwave bursts often have their maxima at frequencies across the spectrum occurring within 1 to 2 min.

The reported peak-flux-densities in the five-minute window were plotted as a function of frequency on log-log graph paper (Figures 1 through 5 and 7 through 9). We considered only frequencies ≥ 200 MHz with the exception of Boulder (184 MHz). Generally the highest observed/reported frequencies were in the 10- to 20-GHz range, although observations at 35 GHz (Sagamore Hill and Nagoya) and beyond (Slough) were available occasionally. Visual fits were made through the plotted points for each event. At frequencies > 2 GHz, it was relatively easy to construct a consensus peak-flux-density spectrum from the plotted points owing both to the smoother spectral and temporal variations at these frequencies and also to the reasonably good (10- to 20-percent variations)^{22,27} inter-calibration of the worldwide patrol. Below 2 GHz, and especially near 200 MHz, the situation becomes more difficult. The narrow band features in the decimeter range present a particular problem since one cannot be sure whether an apparent pronounced spectral variation is real or the result of an erroneous report by a single observatory. The procedure we eventually adopted at decimeter wavelengths was close to a "connect the dots" approach, smoothing out minor variations that could be due to calibration differences but following exactly large variations that we had no reason to doubt. Examples of events with relatively narrow band decimetric features in their spectra are given in Figures 3(b), 3(c), 4(b), 4(c), 7(b), 9(b), and 9(c). At $f \sim 200$ MHz peak-flux-densities reported by different stations observing at closely spaced frequencies can vary by a factor of 2 to 5 or more [Figures 2(a), 4(b), 4(d), 5(a)-5(d), and 7(a)]. It seems doubtful that variations of this size could be due to faulty calibration since the difference would also appear in the daily measurement of the quiet-sun-flux. Rapid spectral variations in the burst emission at these lower frequencies may play a role, although, for certain cases (e.g., Nos. 23, 95, 155), large discrepancies were noted in the reported peak-flux-densities of observatories monitoring the same nominal frequencies. We suggest that the significant differences often observed near 200 MHz result from the effects of different time constants on bursts with fast time structure or from non-linear receiver response for large events. Since both of these effects will tend to reduce observed peak-flux-densities (assuming one does not

27. Tanaka, H., Castelli, J. P., Covington, A. E., Kruger, A., Landecker, T. L., and Tlamicha, A. (1973) Absolute calibration of solar radio flux density in the microwave region, Sol. Phys. 29:243.

over-correct for non-linearity), we favored the higher reported values in events with widely divergent peak-flux-densities at 200 MHz. This decision affected the spectral classifications of 12 events (Nos. 9, 19, 22, 32, 43, 50, 60, 90, 110, 111, 121, and 139) in Table 1.

While observatories may report the times/peak-flux-densities of several maxima at a given frequency in a complex burst, this practice is by no means standard and often only the largest peak is reported. This is a particular problem at the lower (< 1 GHz) frequencies where the largest peak may not occur until late in the event. For certain events with insufficient spectral data at the anchor time, however, it was possible to infer the spectral shape by using peak fluxes reported later (or earlier) in the event as upper limits (Nos. 13, 29, 44, 78, 80, 82, 100, 135, 183, and 186). Also for two cases where a peak 200-MHz flux was reported without a corresponding time (Nos. 6 and 11), we were able to classify the microwave spectrum by assuming that the 200-MHz peak time was the same as that of the peak at the next highest frequency reported (~ 600 MHz in both cases).

For each event in Table 1, we have included a sufficient number of frequency/peak-flux-density pairs to allow one to recreate the spectral curves that we obtained by fitting the tabulated data. In columns 7 through 11, the peak-flux-densities of our constructed spectra at $f = 200$ MHz, 500 MHz, 1 GHz, 3 GHz, and 10 GHz are listed. In columns 12 through 17, frequency/flux-density pairs for the spectral minimum, maximum, and highest frequency reported are listed. If the highest frequency for which observations were reported is less than 10 GHz, the value in column 11 was obtained by extrapolation. For all but 19 cases, indicated by an asterisk in column 17, the information in columns 7 through 17 is sufficient to reconstruct the peak-flux-density spectrum with reasonable accuracy. For the 19 events requiring further data, an additional frequency/peak-flux-density pair is given following the table. The additional data points were needed primarily to describe rapid spectral variations in the decimetric range (300 MHz to ~ 2 GHz). Certain of the events exhibited apparent spectral minima at $f \geq 10$ GHz [e.g., No. 45, Figure 4(a)]; these higher frequency variations are not covered by the data in Table 1. The negative numbers appearing in place of peak-flux-density values in columns 7 through 11 are defined as follows:

- 1 = a station is observing at this frequency but does not report an event,
- 2 = no station is observing,
- 3 = uncertain value but ~ 100 sfu,
- 4 = uncertain value but < 100 sfu,
- 5 = uncertain value.

2.4 Spectral Classes

Despite the occasional complexity that may present itself in the peak-flux-density spectrum of any given event, we found that we were able to classify the spectra of the events in Table 1 into two basic groups and an intermediate type. The dominant spectral type was the U-shape, designated by a 1 in column 18, that comprised 59 percent (113/193) of the sample. For a peak-flux-density spectrum to be classified as U-shaped, we required:

- (a) a spectral maximum ≥ 300 sfu at some frequency $f \geq 2$ GHz,
- (b) a second maximum ≥ 300 sfu at some frequency (≥ 200 MHz)
below that of (a), and
- (c) a spectral minimum at some frequency between that of the
maxima in (a) and (b) (but < 10 GHz) with a flux-density value
significantly (> 40 percent) below those of (a) and (b).

The condition that the minimum occur at $f < 10$ GHz excludes event No. 99²⁸ that has its only minimum at $f \sim 15$ GHz. This is consistent with the specification by Castelli and Barron⁵ that the spectral minimum occur in the decimetric range. Event No. 170 had the highest frequency spectral minimum (5 GHz) of the 113 events that satisfied these criteria. Event Nos. 61, 63, 134, and 187 only marginally met the > 40 percent minimum criterion and are lower-confidence U-bursts.

The above definition allows a variety of spectra to be classified as U-shaped. A number of examples of this spectral type are shown in Figures 1 through 5. Figures 1 and 2 contain examples of the classic U-burst spectrum, with the low frequency flux-density maximum occurring from ~ 200 to 500 MHz. Approximately 75 percent of the U-bursts in our sample had this type of spectrum; ~ 20 percent had their lower frequency maximum in the range from > 500 MHz to 2 GHz. The spectrum in Figure 1(c) has emission maxima in both of these wavelength ranges. Figures 3(a), 3(c), 3(d), and 4(a)-4(d) give seven of the fifteen cases of U-bursts that had their low frequency peak at $f \gtrsim 1$ GHz. The events in Figure 3 were on the list of Castelli and Barron⁵ while those in Figure 4 were not. Figure 5 contains four of the twelve events in our sample that were classified as U-bursts because of our decision to favor high flux values at 200 MHz. Event No. 32 [Figure 5(b)] was also on CB's list.

At this point it is of interest to compare our list of events with U-shaped spectra to that of Castelli and Barron for the period in common from 1966 to 1976. Of the 85 previously identified U-bursts during this period (81 from CB and four

28. Zirin, H., and Tanaka, K. (1973) The flares of August 1972, Sol. Phys.
32:173.

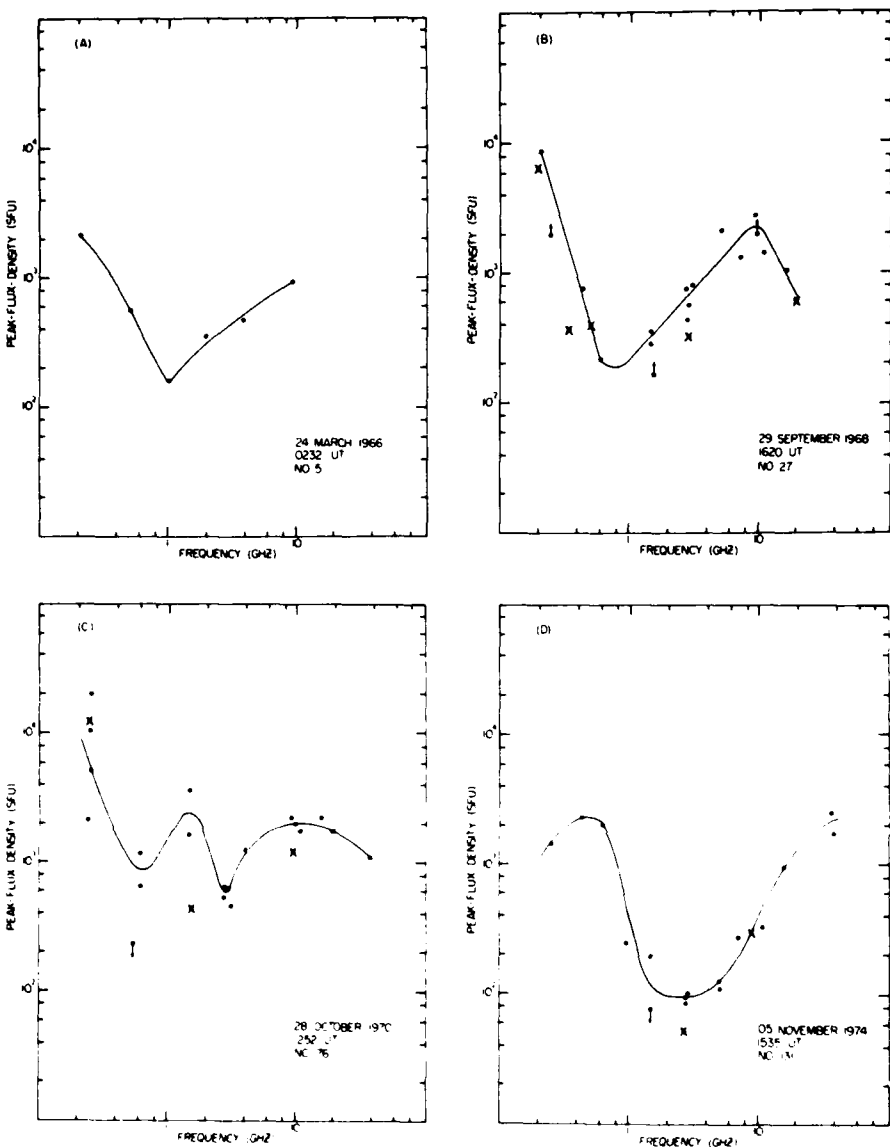


Figure 1. Examples of the Classic U-Shaped Spectrum, With the Low Frequency Maximum Occurring Near 200 MHz. The event on 28 October 1970 (c) had an additional maximum in the decimetric range. Each of these events was on Castelli and Barron's⁵ list of U-bursts. In Figures 1 through 5 and 7 through 9, Xs indicate doubtful or uncertain flux density values and downward (upward) pointing arrows indicate upper (lower) limits. Uncertainties in measured peak fluxes at frequencies > 2 GHz are typically $\leq \pm 20$ percent. Differences in reported values at $f \lesssim 2$ GHz may be substantially larger (factors of 2 to 10) as can be seen from these figures. Note that the origin of the y-axis of the plots in Figures 1 through 5 is at 10 sfu vs 1 sfu in Figures 7 through 9

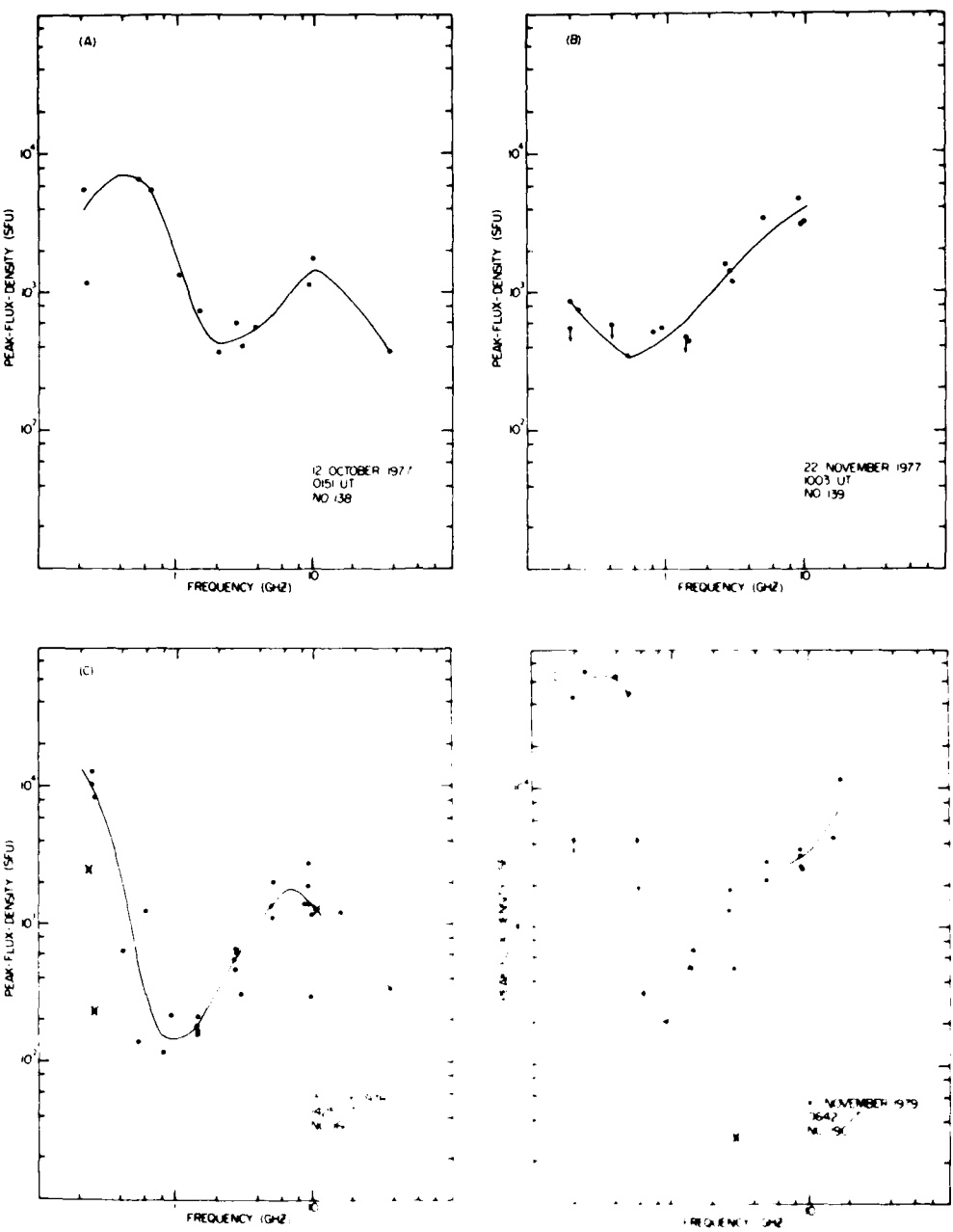


Figure 2. Examples of the Classic U-Shaped Spectrum With the Low Frequency Maximum Occurring Near 200 MHz. These events occurred after the period examined by Castelli and Barron.⁵ The U-burst on 22 November 1977 (b) was one of 12 events in Table 1 whose peak-flux-density classification was affected by our decision to favor higher reported flux values at $f \sim 200$ MHz.

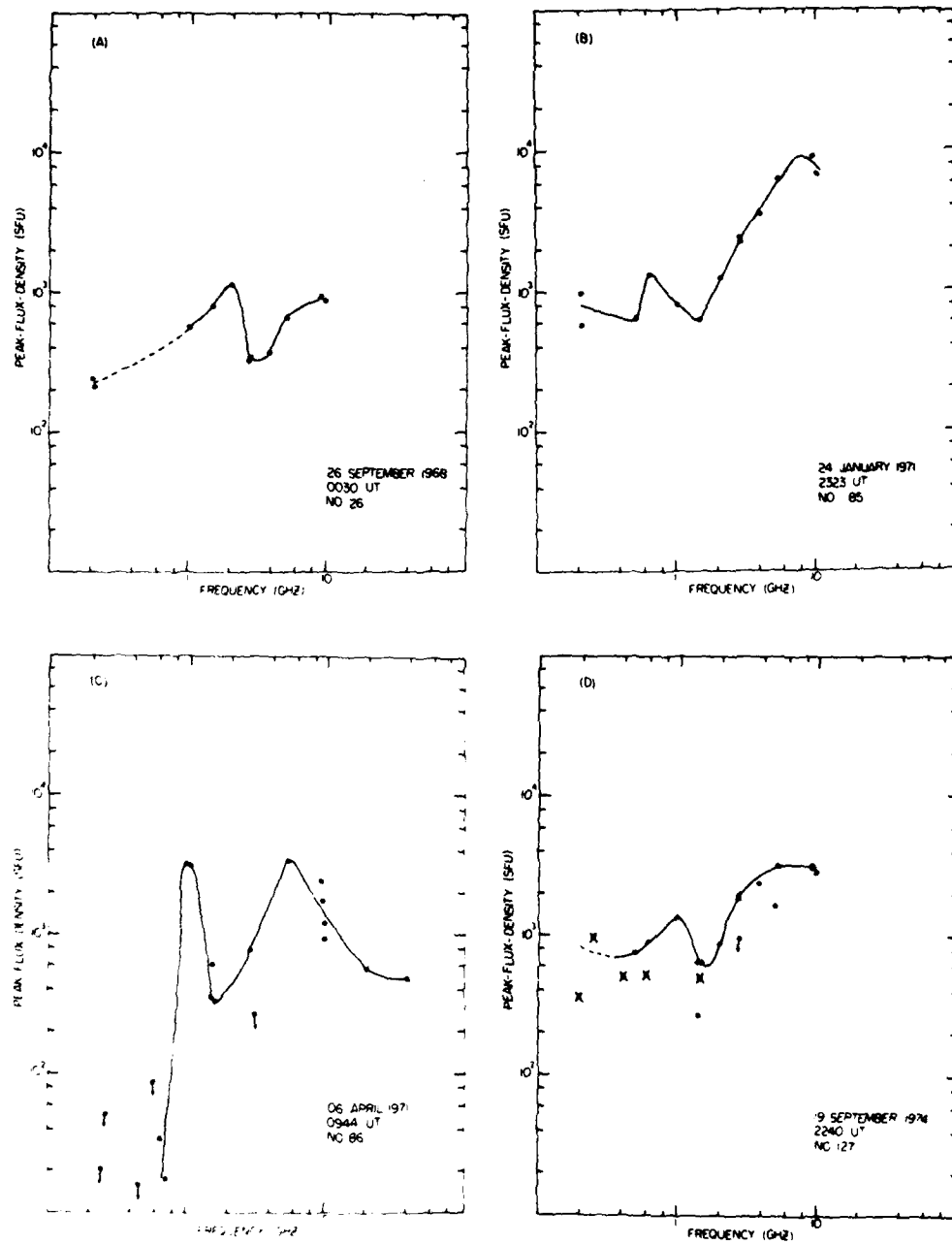


Figure 3. Examples of U-Shaped Peak-Flux-Density Spectra That Had Their Lower Frequency Maximum in the Decimetric Range. Each of these events was on Castelli and Barron's⁵ U-burst list

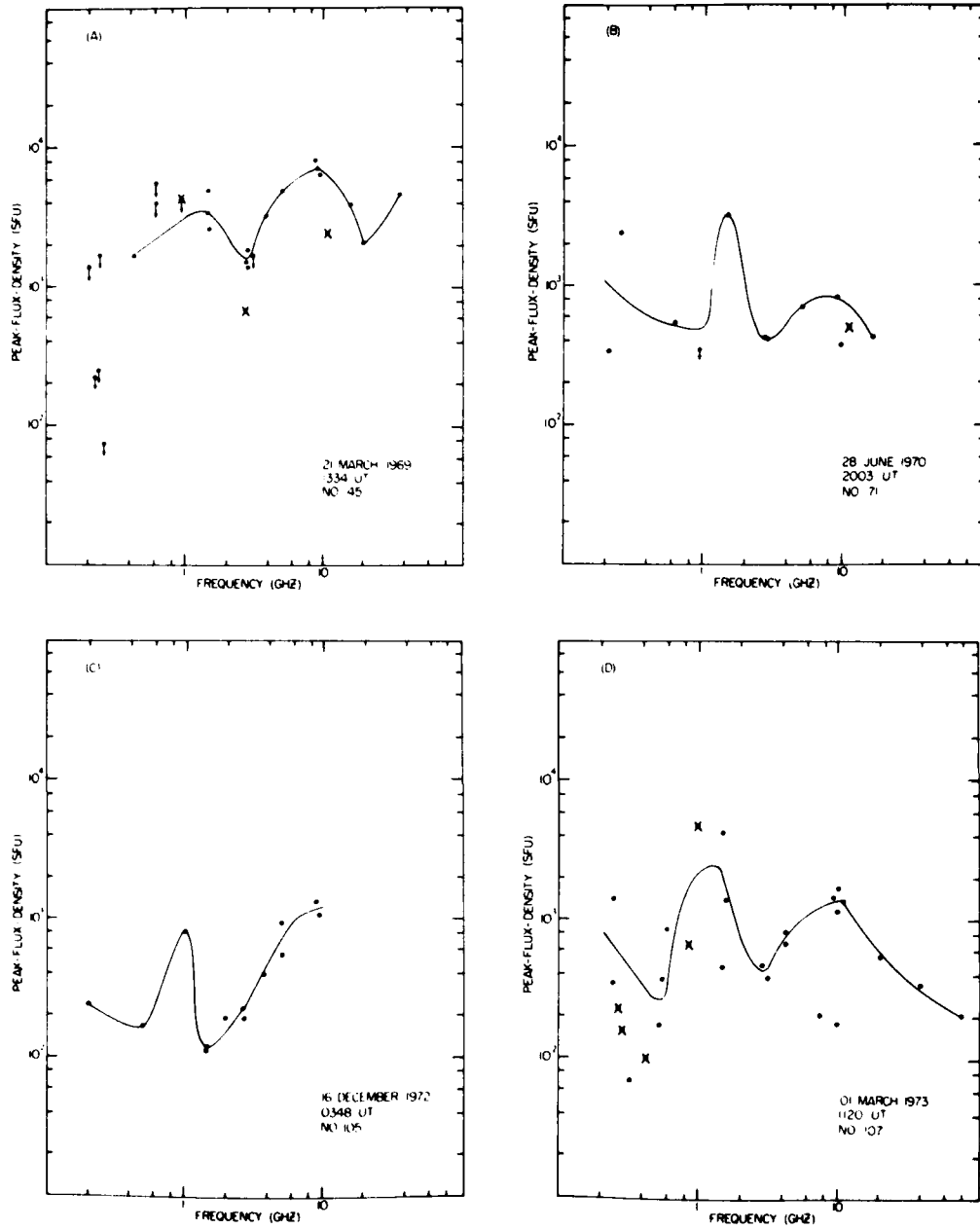


Figure 4. Examples of U-Shaped Peak-Flux-Density Spectra That Had Their Lower Frequency Maximum in the Decimetric Range. These events were not on Castelli and Barron's⁵ list

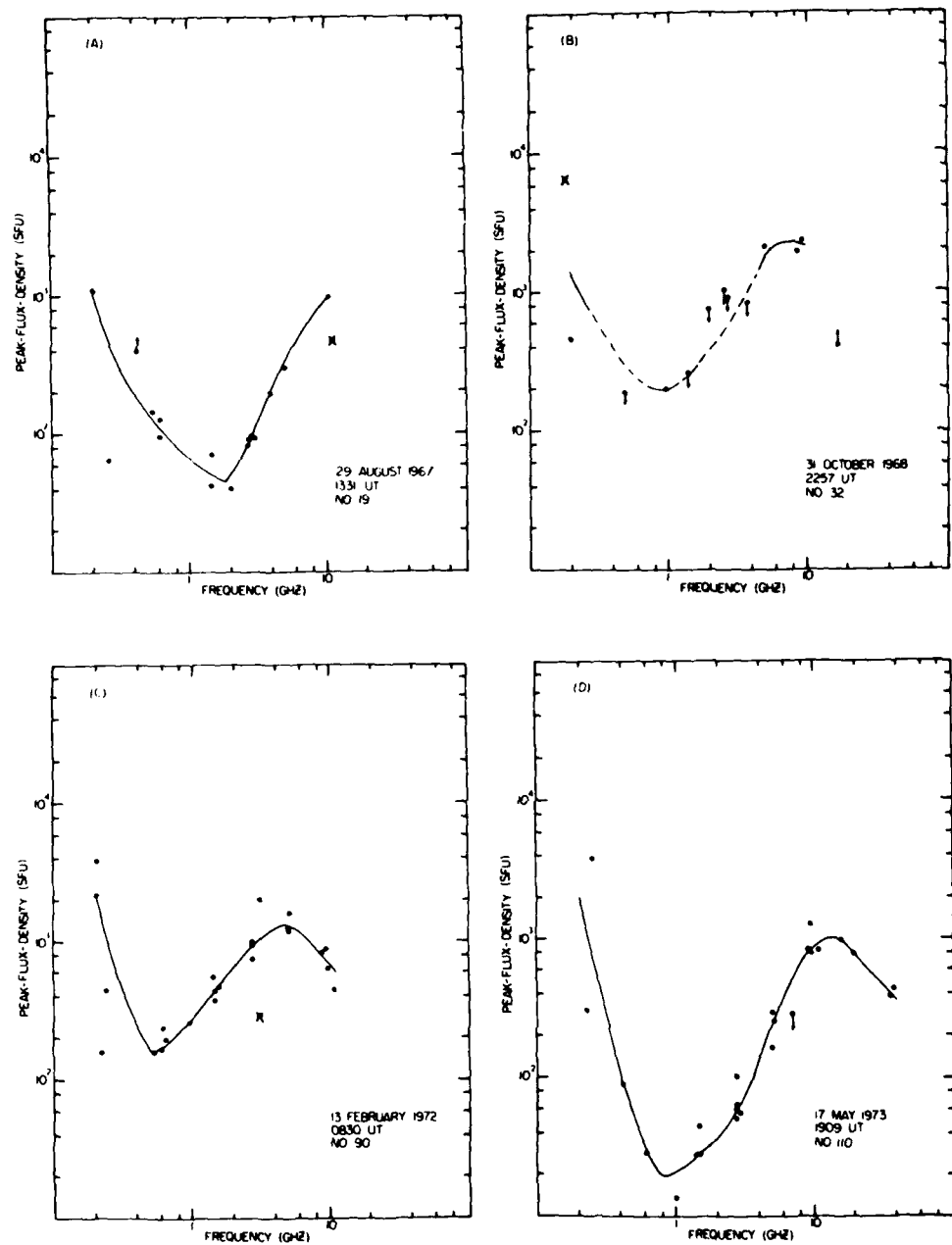


Figure 5. Four of the Ten Events in Table 1 That Were Classified as U-Bursts Because of Our Decision to Favor High Flux Values at 200 MHz. The event on 31 October 1968 (b) was also classified as a U-burst by Castelli and Barron⁵

added by Castelli and Tarnstrom,⁶ 11 occurred either at or behind the solar limb ($\phi > 85^\circ$) and were not considered for our list. For event No. 10 (02 November 1967, 0856 UT) on the CB list, no observatory on patrol reported an event with $Sp \geq 800$ sfu [Gorky, $Sp(9.4\text{ GHz}) > 520$ sfu]. For 14 other events on CB's list (several of which were discussed in the introduction), we were either unable to classify the peak-flux-density spectrum because of insufficient data in the five-minute window (nine cases) or arrived at a different classification (five cases). Thus there were 59 events in the intersection of our U-burst data sets for the common years of these studies. In addition, we identified 25 events during this period, not included on the U-burst list compiled by CB and Castelli and Tarnstrom, that satisfied the U-shaped spectral criteria we adopted. We point out that 13 of these 25 events (Nos. 3, 4, 19, 49, 50, 63, 66, 67, 71, 75, 105, 110, and 111) would not have been classified as U-bursts if spectral maxima ≥ 1000 sfu (vs ≥ 800 sfu) in the meter/decimeter and centimeter wavelength ranges had been required. This would account for their absence from the CB list. (By the same standard, event Nos. 5, 7, and 26 in Table 1 might be excluded from the CB list.) The 12 events that appear to satisfy their criteria and are missing from their list are Nos. 6, 12, 37, 45, 61, 83, 90, 94, 97, 107, 112, and 133.

Figure 6 is a histogram showing the timing of the flux-density peak at 200 MHz relative to that of the 10-GHz peak for the U-bursts in Table 1. Only cases where reported maxima at both of these frequencies fell within the five-minute

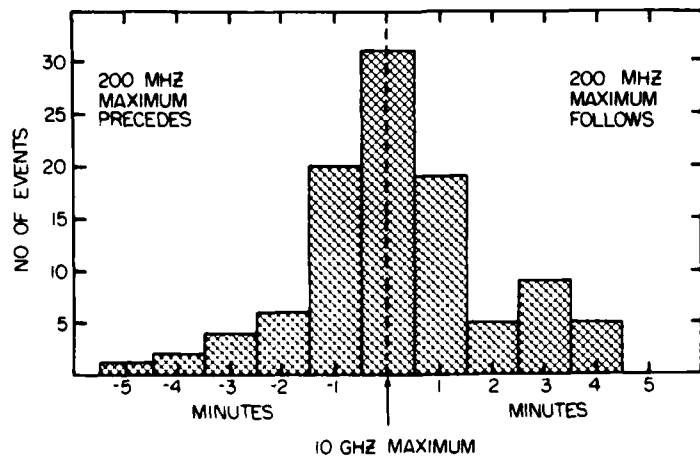


Figure 6. The Timing of the Maximum ~ 200 -MHz Emission for the U-Bursts in Table 1 Relative to the Timing of the ~ 10 -GHz Maximum. For ~ 70 percent (70/102) of the cases the peaks at these widely separated frequencies occur within ± 1.5 min of each other. The data are taken from columns 3 and 4 in Table 1

sliding window were considered. The histogram shows that intensity maxima at these widely spaced frequencies often occur quite close in time, within ± 1.5 min for ~ 70 percent (70/102) of the cases.

For 52 of the 165 events in Table 1 for which we were able to determine spectra, a ≥ 800 -sfu maximum at $f \geq 2$ GHz was not accompanied by a maximum with $S_p \geq 800$ sfu at a lower frequency. In many cases the high frequency emission was apparently unaccompanied by any emission at lower frequencies and emission would appear to taper smoothly down from the centimeter wavelength maximum and cut off at frequencies $\gtrsim 1$ GHz. In other cases the spectrum was U-shaped but the lower frequency maximum did not have $S_p \geq 800$ sfu. Still in a few other cases the spectrum below the centimeter wavelength peak neither cut off completely nor turned back up, but remained relatively flat at a given flux density level. To distinguish between these various types of events we adopted the following classification scheme. We classified as having intermediate peak-flux-density spectra those events for which:

- (a) a spectral maximum ≥ 800 sfu occurred at $f \geq 2$ GHz,
- (b) no significant ($S_p \geq 800$ sfu) spectral maximum occurred at a frequency lower than that of (a) (down to 200 MHz), and
- (c) S_p (200 MHz) ≥ 100 sfu.

This set of criteria distinguishes these events from those having cutoff or quasi-cutoff spectra for which criteria (a) and (b) also apply, but for which criterion (c) becomes: S_p (200 MHz) < 100 sfu. Thus microwave bursts of the intermediate spectral class, designated by a 2 in column 18, have peak 200-MHz emission between that of U-bursts and cutoff events (3 in column 18). We point out, however, that the occurrence of a decimeter wavelength peak with $S_p \geq 800$ sfu automatically qualified an event as a U-burst in our classification scheme (assuming it met the other stated criteria), regardless of the peak-flux-density of any reported 200-MHz burst.

While for many of the events having cutoff spectra, emission appeared to be cut off well above 200 MHz, we know from experience that, because of the relatively high level of activity at the lower frequencies, many and perhaps a majority of the smaller events ($S_p < 100$ sfu) at 200 MHz go unreported.²⁹ Thus the cutoff events are not necessarily those for which no low frequency emission was observed, but rather are events for which the peak 200-MHz emission was significantly down (a factor of eight or more) from its centimeter wavelength maximum. In all cases where no event was reported near 200 MHz (184 to 328 MHz),

29. Roelof, E. C., Dodson, H. W., and Hedeman, E. R. (1983) Dependence of radio emission in large $H\alpha$ flares 1967 - 1970 upon the orientation of the local solar magnetic field, Sol. Phys. 85:339.

we checked the published patrol times to see if a station (e.g., Hiraiso, Gorky, Sagamore Hill) was, in fact, observing in this frequency range. If a station was observing and did not report an event, we assumed that S_p (~ 200 MHz) < 100 sfu. No station was observing near 200 MHz for event No. 165, and we could not classify its spectrum by our method.

Eighteen of the 193 events in our data set (nine percent) had intermediate peak-flux-density spectra and 34 (18 percent) had cutoff spectra. Examples of intermediate spectra are shown in Figure 7 and examples of cutoff spectra are given in Figures 8 and 9. Examples of intermediate and cutoff spectra with decimetric peaks are shown in Figure 7(b), and Figures 9(b) and 9(c), respectively.

We were unable to classify the peak-flux-density spectra of 28 (15 percent) of the events in our data sample (? in column 18). The most common reason (20 cases) for our inability to construct a meaningful spectrum was the lack of data points, particularly at low frequencies, within the five-minute sliding window. For five other events (Nos. 1, 20, 21, 128, and 172), burst maxima within the five-minute window were reported across the spectrum, but the peak-flux-density values at ~ 200 MHz, on which our classification system hinges, were uncertain and were < 800 sfu. [Because we favored high reported flux values at lower frequencies, we classified four events (Nos. 11, 32, 92, and 169) with doubtful ~ 200 -MHz flux values > 800 sfu as U-bursts.] For two cases (Nos. 119 and 136), unresolvable discrepancies in reported flux values at one or more frequencies made it impossible to assign a classification. Note that criterion (a), requiring a spectral maximum ≥ 800 sfu at $f \geq 2$ GHz, is the same for all three spectral classes. Only one event in Table 1 did not satisfy this requirement and fell into the unclassified category. Event No. 30 had a single spectral maximum at 60% MHz of 260,000 sfu; emission declined to a value of 220 sfu at 19 GHz, the highest frequency at which observations were reported.

2.5 Associated Sweep Frequency Meter Wavelength Events

The starting times of meter wavelength Type II sweep frequency bursts, associated with the large microwave bursts under consideration, are given in column 19 of Table 1, and the occurrence of an associated Type IV burst is indicated by an X in column 20. To determine the Type II onset (and end) times that are used in the analyses in the next section, we preferentially used the meter wavelength times reported by Ft. Davis, Culgoora or Weissenau. If two of these stations reported an event, we averaged the reported times. However, if one of these three stations was on patrol and did not report a Type II burst and another station (e.g., Durnten or Sagamore Hill) did, we considered the Type II report to be valid. Also, if no meter wavelength Type II or IV was observed but an event

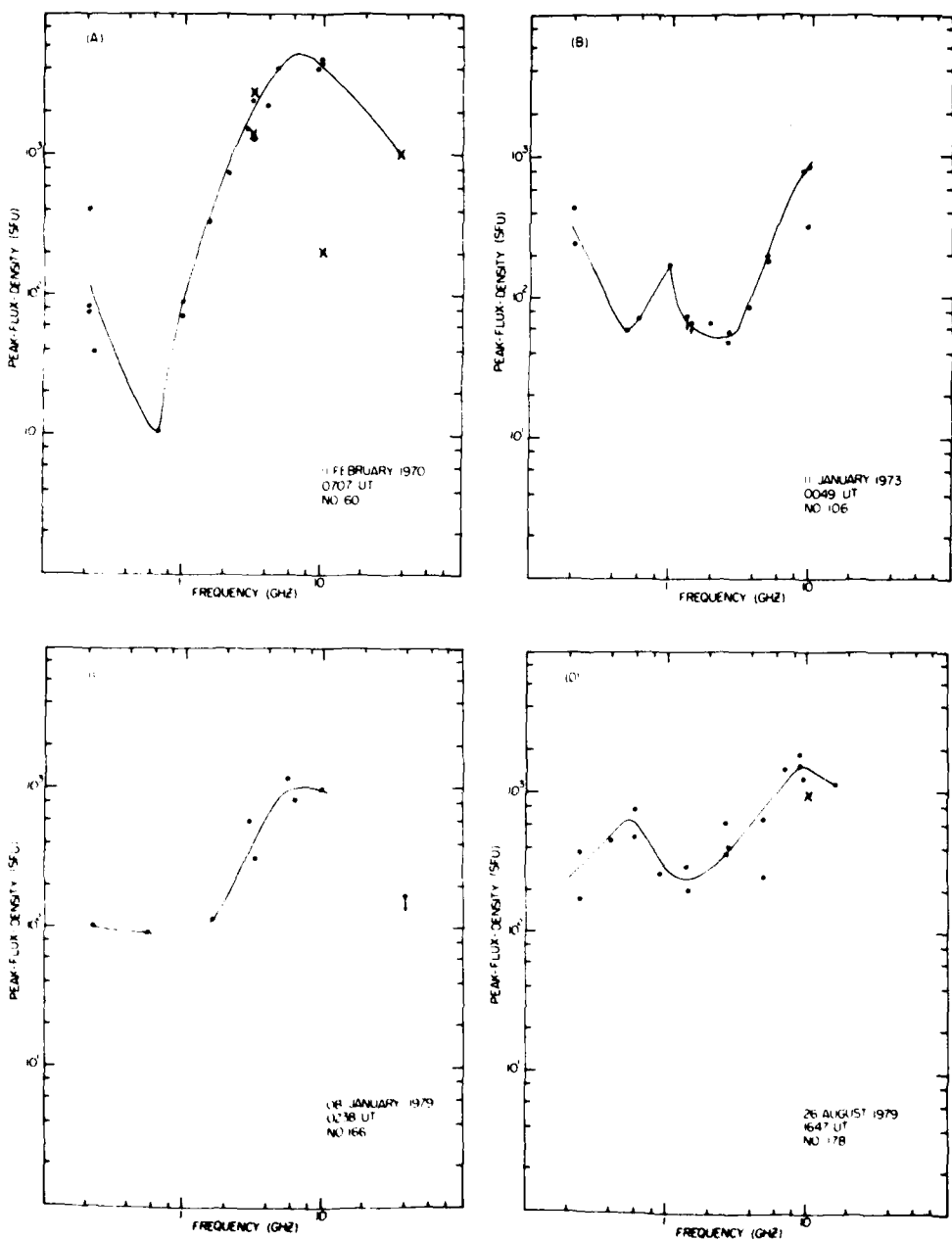


Figure 7. Examples of Microwave Bursts With What We Have Termed "Intermediate" Peak-Flux-Density Spectra. The classification of the event on 11 February 1970 (a) was affected by our decision to favor the higher reported flux values near 200 MHz. The spectrum of the event on 11 January 1973 (b) has a decimetric component, while that of 08 January 1979 (c) is relatively flat in the meter and decimeter range

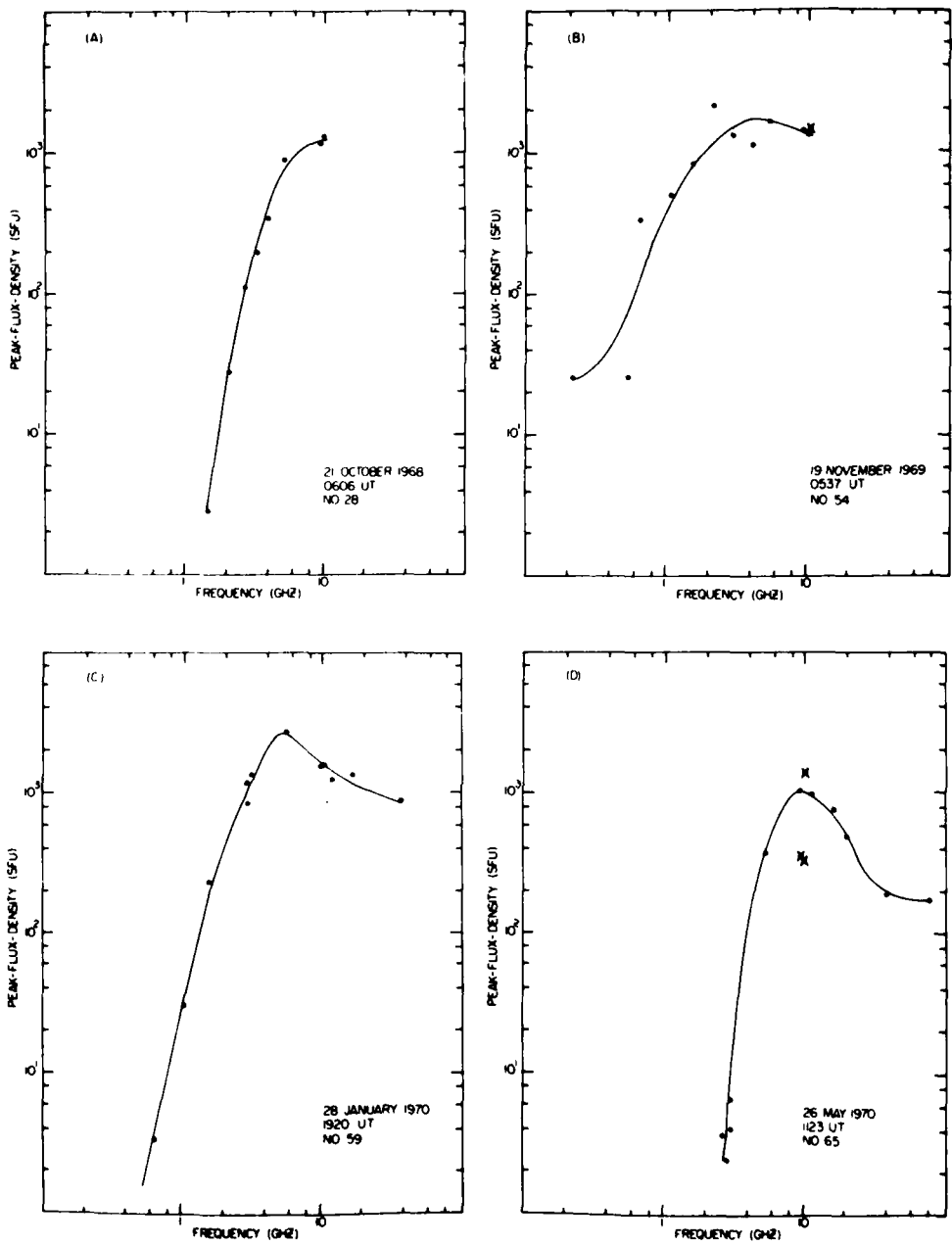


Figure 8. Examples of Large Microwave Bursts With Cutoff or Quasi-Cutoff Spectra

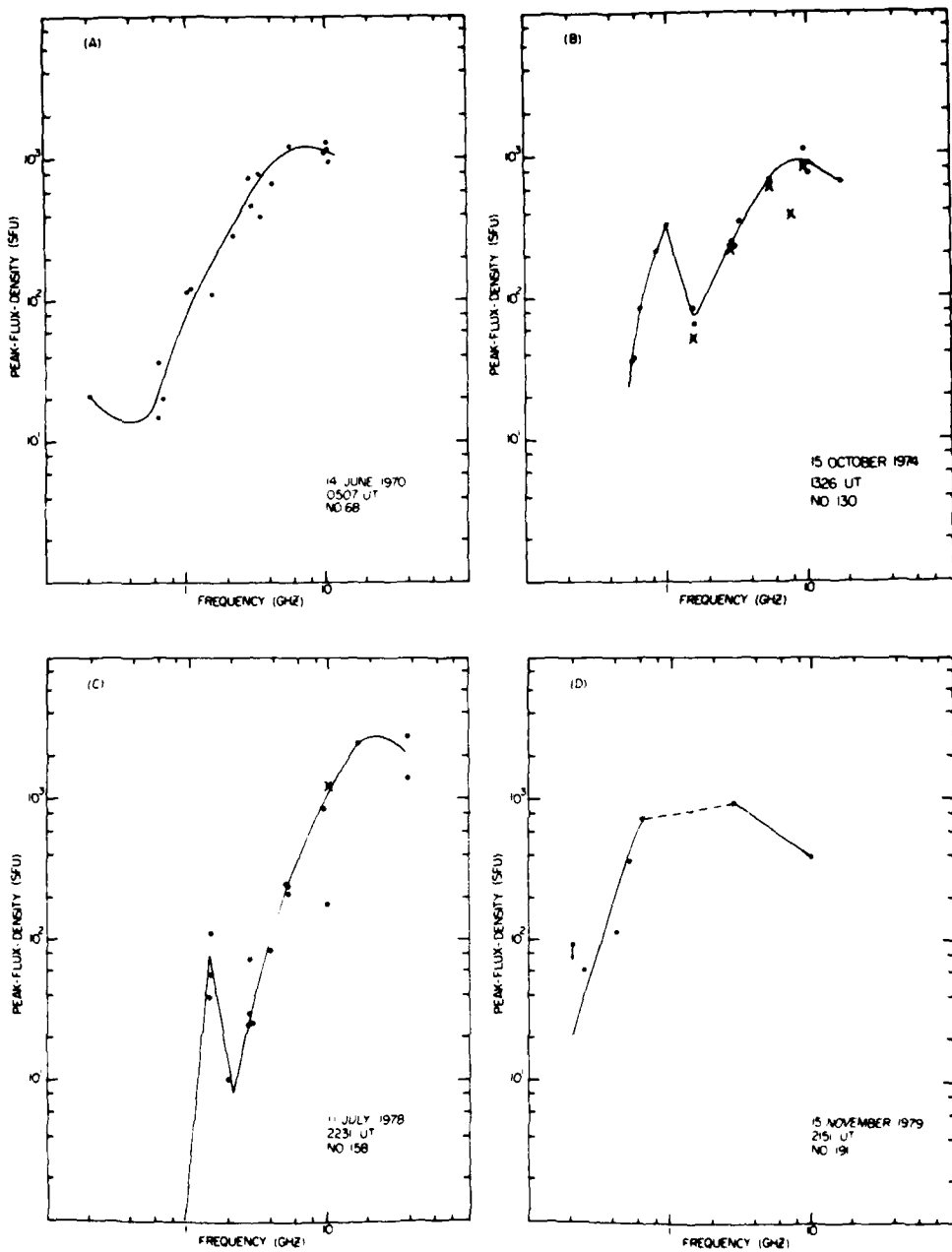


Figure 9. Examples of Large Microwave Bursts With Cutoff or Quasi-Cutoff Spectra. The events on 15 October 1974 (b) and 11 July 1978 (c) exhibited a decimetric component in their spectra

was reported at decimeter (c) or decameter (k) wavelengths, we have indicated so by appending a c or a k to the entries in columns 19 and 20 as appropriate. For the Type IV associations, we did not consider events for which continuum (but not Type IV) was reported.

Meter wavelength Type III associations are indicated in column 21 by an X (with c and k appended as in columns 19 and 20). We considered a Type III event to be associated with a listed microwave burst if Type III emission, reported by any observatory, occurred within ± 10 min of the listed time of the 10-GHz emission maximum. We considered long duration (S or N) Type III activity to be associated only if it began within ± 15 min of the 10-GHz maximum. The s descriptor (for "simultaneous") was used when the Type III duration encompassed the time of the 200-MHz maximum, ended ≤ 0.5 min prior to the 200-MHz maximum, or began ≤ 0.5 min after it. Of course, as Svestka and Fritzova-Svestkova²¹ point out, it is impossible to tell if Type III emission and the 200-MHz maximum are exactly coincident, without examining the sweep frequency records, for the typical case for these large bursts of a Type III series lasting for several minutes and composed of tens of individual bursts.

We used QBSA and SGD as sources for the sweep frequency data. In columns 19 through 21, N.O. (no observations) indicates events for which sweep frequency data were not available.

2.6 Proton Data

For the proton associations for the events in Table 1, we used the Catalog of Solar Particle Events, 1955-1969,³⁰ reports by Dodson et al,^{31,32} and the published list of van Hollebeke et al³³ for the years 1965 through 1972. We made the associations ourselves for the subsequent years. In column 21, we have listed the characteristic of the logarithm of the peak prompt (i.e., non-sudden commencement associated) $\cdot 10$ -MeV proton flux [$J (\cdot 10 \text{ MeV}) \text{ in pr cm}^{-2} \text{ sec}^{-1} \text{ sr}^{-1}$] for each event with proton association. We only considered increases for which

-
30. Svestka, Z., and Simon, P., Eds. (1975) Catalog of Solar Particle Events, 1955 - 1969, D. Reidel Pub. Co., Dordrecht, Holland.
 31. Dodson, H. W., Hedeman, E. R., and Mohler, O. C. (1977) Survey and Comparison of Solar Activity and Energetic Particle Emission in 1970, AFGL-TR-77-0222, AD A048479.
 32. Dodson, H. W., Hedeman, E. R., and Mohler, O. C. (1978) Solar and Geophysical Associations With the Principal Energetic Particle Events in 1971 and 1972, AFGL-TR-78-0266, AD A065260.
 33. van Hollebeke, M. A. I., Ma Sung, L. S., and McDonald, F. B. (1975) The variation of solar proton energy spectra and size distribution with helio-longitude, Sol. Phys. 41:189.

the logarithm of the peak near-Earth > 10 -MeV flux had a characteristic ≥ -2 . Somewhat smaller increases, with $\log(J) < -2$, can be observed by existing satellite sensors, but fluctuations at this level are common, and it is difficult to confidently associate these small increases with flares.^{26,33} For the period from January 1965 to May 1967, we relied on the proton event classification of Smart and Shea³⁴ as used in Svestka and Simon³⁰ to determine the logarithm of $J (> 10 \text{ MeV})$. For the period from May 1967 to May 1973, we were able to make this determination directly from the > 10 -MeV data acquired by the Johns Hopkins University/Applied Physics Laboratory (JHU/APL) experiments aboard IMP F, G, and I and published in SGD. For the years 1973 to 1979, we worked with the 20- to 40-MeV data collected by the JHU/APL sensors aboard IMP H and J. For this differential channel, a peak flux of $\geq 10^{-4} \text{ pr cm}^{-2} \text{ sec}^{-1} \text{ sr}^{-1} \text{ MeV}^{-1}$ corresponds to a peak > 10 -MeV flux of $J \geq 10^{-2} \text{ pr cm}^{-2} \text{ sec}^{-1} \text{ sr}^{-1}$ if one assumes a spectral slope of -3 .³³ In all cases we subtracted the background due to earlier events when determining $\log(J)$.

Since: (1) prominent flares from complex active regions tend to be closely grouped in time (e.g., the August 1972 region where four major flares occurred in a five and one-half day period), (2) big flares tend to produce big proton events, and (3) large proton events have durations ranging from tens of hours to days, it is not surprising that many of the events in Table 1 occurred when a proton event, perhaps associated with an earlier listed event, was already in progress. In some of these cases a fresh injection of protons can be seen above the enhanced background. In other cases no new injection of protons is evident. In these latter cases, we have indicated that a possible event was masked by putting an M in column 21. The number in parentheses following the M is the characteristic of the logarithm of the enhanced > 10 -MeV flux at the time of the listed microwave event. For several events in Table 1, an apparently associated proton event may have, in fact, been caused by another flare (or flares) occurring closely in time. (Or, alternatively, several flares may have contributed to the peak proton flux.) This is a particular problem for proton events originating in eastern hemisphere activity, since these particle events tend to have longer rise times.³⁵ In column 21, we have denoted these "ambiguous" flare proton event associations with an A. The number in parentheses following the A is the characteristic of the logarithm of the peak prompt > 10 -MeV flux. It is important to note that not all parent-flare

34. Smart, D. F., and Shea, M. A. (1971) Solar proton event classification system, Sol. Phys. 16:484.

35. Reinhard, R., and Wibberenz, G. (1974) Propagation of flare protons in the solar atmosphere, Sol. Phys. 36:473.

candidates that might have produced a given A event are necessarily listed in Table 1, but only those that met our selection criteria.

We note that for the period May 1967 to May 1973, Svestka and Simon³⁰ and Dodson et al^{31,32} listed several events in Table 1 as sources of low energy (< 10 MeV) proton events [Nos. 6 (spectral class = 1), 63 (1), 72 (1), and 80 (3)], high energy (> 10 MeV) events with low ($< 10^{-2} \text{ pr cm}^{-2} \text{ sec}^{-1} \text{ sr}^{-1}$) fluxes [81 (1)], or high energy events only observed by satellites far removed ($> 60^\circ$) from the Earth-sun line [56 (3) and 84 (?)]. For these events, we have placed a "--" or an M (followed by the masking flux) in column 21 depending on whether the pre-event level was at quiet background or an event was in progress.

2.7 Major Proton Events, 1965-1979

By examining the proton association of the 113 U-bursts in Table 1, we can determine a false alarm rate for the U-burst forecast tool for predicting proton events above a given threshold. However, since some major proton events may be associated with flare-bursts without U-shaped spectra, or may have Sp (≥ 2 GHz) < 800 sfu,^{6,19} it is not possible to determine from Table 1 the fraction of proton events of a given peak intensity that will be associated with U-bursts. In order to determine this parameter, we have compiled the data in Table 2 for the 46 prompt proton events with $J (> 10 \text{ MeV}) \geq 10 \text{ pr cm}^{-2} \text{ sec}^{-1} \text{ sr}^{-1}$ (above pre-event background) occurring from 1965 to 1979 that had unambiguous visible hemisphere ($85^\circ E \geq \phi \leq 85^\circ W$) parent H α flare associations. This is the same list of events that was used in the study by Cliver et al.,¹⁹ but was not published there. The $J (> 10 \text{ MeV}) \geq 10 \text{ pr cm}^{-2} \text{ sec}^{-1} \text{ sr}^{-1}$ threshold was selected because it is currently in use at the NOAA Boulder forecast center.⁷ Columns 2 and 3 in Table 2 give the flare date and location. Columns 4 and 5 give the times of the associated Type II and Type IV bursts, respectively. In column 6, the peak-flux-density and the time of its occurrence at 200 MHz (184 to 328 MHz) are given. This is not a consensus or averaged value of the flux near the frequency, but is the highest flux value reported by any observatory on patrol in this frequency range during the time of the H α flare. This is also the case for column 7 where the maximum flux density reported by any observatory in the 10-GHz range (8.2 to 11.8 GHz) is listed along with the time of its occurrence. A "--" in columns 4 and 5 indicates that no event was reported; an N.O. means that the appropriate observations were not made. In column 8, a U denotes those flare-bursts that had U-shaped spectra satisfying the criteria used in Table 1, while a 40 indicates proton events with $J (> 10 \text{ MeV}) \geq 40 \text{ pr cm}^{-2} \text{ sec}^{-1} \text{ sr}^{-1}$.

Table 2. Large Proton Events 1965-1979 With Unambiguous Visible-Disk-Flare Associations

DATE (2)	FLARE LOCATION (3)	TYPE II (4)	TYPE IV (5)	200 MHZ		10 GHZ (7)	U/(J>40) (8)
				MAX FLUX/TIME (6)	MAX FLUX/TIME (7)		
1. 05 Feb 65	N08 W25	-	(a) 1800-1940	>250/?	9/1831	--	
2. 24 Mar 66	N20 W42	0234-0253	? (b)	2090/0234	930/0232	U/40	
3. 07 Jul 66	N35 W48	0038-0114	0042-0200	950/0039	12750/0038	U/40	
4. 28 Aug 66	N22 E04	1531-1548	1527-1640	(70000)/1527	3580/1528	U/-	
5. 02 Sep 66	N22 W58	0554-0614	-	5000/(0556)	6970/0556	U/40	
6. 23 May 67	N27 E28	1838-1905	1839-2320	N.O.	23000/1947	U/40	
7. 28 May 67	N28 W33	0539-0556	-	3600/0540	7300/0542	U/40	
8. 09 Jun 68	S14 W08	-	0839-0940c	6800/0848	1360/0850	U/40	
9. 29 Sep 68	N17 W52	1619-1639	1636-1650	8700/1620	2810/1620	U/-	
10. 04 Oct 68	S16 W37	0000-0027	- *	(2170)/2359	85/0020	--	
11. 31 Oct 68	S14 W37	2359-0005	0002-0035	790/0009	2000/0011	U/40	
12. 01 Nov 68	S18 W47	0852-0900	0853-0915c	175/(0841)	1930/0912	-/40	
			0925-0952c				
13. 25 Feb 69	N13 W37	-	0904-1130	80000/0915	6600/0912	U/40	
14. 26 Feb 69	N13 W46	0426-0441	- *	>1360/0426	3670/0425	U/-	
15. 27 Feb 69	N13 W65	1404-1426	1407-1450	3750/1405	3000/1408	U/-	
16. 07 Jun 69	N11 E34	-	0953-0959c	55/0956	245/0956	--	
17. 25 Sep 69	N14 W14	-	- *	400/0834	17/0753	--	
18. 31 Jan 70	S23 W62	1518-1522	1536-1614	137/1807	33/1601	--	
19. 07 Mar 70	S14 E48	-	-	-	42/1126	-/40	
20. 29 Mar 70	N13 W37	0040-0053	0038-0300	>13300/0103	5600/0041	U/40	
21. 30 May 70	S08 W32	-	- *	300/0315	30/0340	--	
22. 23 Jul 70	N09 E09	-	1836-1903	8000/1934	4200/1845	U/-	
			1918-1936				
			1946-1957				
23. 05 Nov 70	S12 E36	0324-0351	0325-0450	470/0339	1250/0327	--	
24. 24 Jan 71	N18 W49	2316-2342	2317-0250	1000/2320	9100/2323	U/40	
25. 06 Apr 71	S19 W80	N.O.	N.O.	50/0941	2300/0944	U/40	
26. 04 Aug 72	N14 E08	-	0621-1245	(500000)/0642	36500/0627	U/40	
27. 07 Aug 72	N14 W37	1519-1602	1517-1540	(8500)/1516	27056/1522	U/40	
28. 29 Apr 73	N14 W73	2101-2122	2100-2250	16700/2216	11897/2103	U/-	
29. 07 Sep 73	S18 W46	1200-1207k	1155-1200k	610/1141	334/1200	--	
			1207-1215k				
30. 04 Jul 74	S16 W08	1359-1407	1353-1446	105000/1408	4950/1354	?/-	
31. 10 Sep 74	N10 E61	2136-2158	2134-2220	3850/2143	9700/2141	U/40	
32. 19 Sep 74	N09 W62	2233-2310	2232-0045	(968)/2238	3300/2240	U/40	
33. 05 Nov 74	S12 W78	1536-1551	1545-1700	1421/1535	321/1535	U/40(c)	
34. 30 Apr 76	S08 W46	2106-2128	2105-0055	897/2103	3188/2108	U/40	
35. 16 Sep 77	N07 W20	2233-2247	2230-0025	(2500)/2400	900/2308	?/40	
36. 19 Sep 77	N08 W57	1038-1044	1042 1130	325/0950	2239/1037	U/40	
37. 22 Nov 77	H24 W40	-	1002-1045	1600/1035	4735/1004	U/40	
38. 13 Feb 78	H16 W18	0138-0200	0134-0400	300/0152	317/0202	-/40	
39. 11 Apr 78	N22 W56	1359-1425	1350-1449	770/1405	1318/1354	U/40	
40. 28 Apr 78	N22 E38	1320-1331	1319-1540	143600/1323	8728/1329	U/40	
41. 07 May 78	N23 W72	0328-0355	0329-0715+	15000/0329	3450/0329	U/40	
42. 22 Jun 78	N18 E16	1704-1724	1703-1756	1150/1706	75/1742	--	
			1735-1748				
43. 23 Sep 78	N35 W50	0958-1028	0954-1100	3850/1001	682/1002	-/40	
44. 09 Oct 78	S14 W61	1959-2016	- *	4060/1950	415/1951	--	
45. 21 Aug 79	N17 W40	0615-0645	0608-0620c	51/0613	27/0618	-/40	
46. 15 Nov 79	N29 W35	2147-2206	2145-2235	90/2144	634/2151	-/40	

Table 2. Large Proton Events 1965-1979 With Unambiguous Visible-Disk-Flare Associations (Contd)

Notes:

- (a) Ft. Davis reported unclassified bursts with Type II characteristics, 1800 to 1811 UT.
 - (b) Type IV emission began at 0300 UT, ~ 2 hr before the H α onset of the listed flare, and continued until 0523 UT.
 - (c) The high frequency spectral maximum occurred at $f \geq 35$ GHz ($S_p \sim 2000$ sfu).
- * Continuum or Type I activity, beginning during the listed flare, was reported for these events.

3. DATA ANALYSIS

3.1 Peak-Flux-Density Spectral Type vs Proton Events

In Table 3 we present our results on the association of proton events with large radio bursts of different spectral types for the events in Table 1. Since it is well known and understood in terms of interplanetary propagation that the protons accelerated in western hemisphere flares are more likely to be observed near Earth than those with an eastern hemisphere origin, we have divided the table into two parts, (a) and (b), corresponding to western- and eastern-hemisphere events, respectively. We have further divided the events from each hemisphere into clean and masked or ambiguous cases. The clean events are those in which the flare association is unambiguous, and a fresh injection of > 10-MeV protons is observed above the flux background, either quiet or disturbed, existing at the time of the flare.

Considering the clean cases only, the percentage association of protons with the three spectral types is as follows:

<u>Spectral Type</u>	<u>West</u>	<u>East</u>	<u>Total</u>
(1) U-burst	91% (31/34)	64% (25/39)	77% (56/73)
(2) Intermediate	71% (5/7)	75% (3/4)	73% (8/11)
(3) Cutoff	75% (3/4)	18% (2/11)	33% (5/15)

The high degree of association between U-bursts and proton events for western hemisphere flares supports the evidence presented by Castelli and Barron,⁵ indicating that the U-burst is an almost sufficient condition for the occurrence of a

Table 3. Peak-Flux-Density Spectral Class vs Proton Event Size

(A) WESTERN HEMISPHERE

LOGARITHM OF >10 MEV PEAK FLUX SPECTRAL TYPE	"CLEAN" CASES						AMBIGUOUS or MASKED EVENTS				
	≥2	1	0	-1	-2	<-2	≥2	1	0	-1	-2
U - SHAPED	10	12	4	3	2	3	2	6	3	4	2
INTERMEDIATE			2	2	1	2	1	1	1	1	1
CUT - OFF			1	2		1	1	2	5		
UNCLASSIFIED	1	2		1			1	2	3	1	

(49) (36)

(B) EASTERN HEMISPHERE

LOGARITHM OF >10 MEV PEAK FLUX SPECTRAL TYPE	"CLEAN" CASES						AMBIGUOUS or MASKED EVENTS				
	≥2	1	0	-1	-2	<-2	≥2	1	0	-1	-2
U - SHAPED	2	4	4	7	8	14	1	1	6	7	8
INTERMEDIATE			1		2	1	1	2			
CUT - OFF				1	1	9	3	3	2	3	
UNCLASSIFIED	1	1	1	1	1	4	1		2	6	

(62) (46)

proton event of any size. However, we note that the large western hemisphere flare-bursts with intermediate and cutoff spectral classifications also have significant proton association (71 and 75 percent, respectively). Since the number of western hemisphere events of these two spectral types is small, it may be appropriate to increase our sample size by considering the percentage association of the three spectral types with protons for flares occurring anywhere on the visible disk ($85^{\circ}\text{E} \geq \phi \leq 85^{\circ}\text{W}$). As expected, the percentage association for U-bursts is smaller when the whole sun is considered. It is significantly below the 97 percent (70/72) association found by Castelli and Barron for the visible disk. [We note that the full sun association increases to 82 percent (60/73) if one includes the four low energy/low flux proton events that were linked to U-bursts (Section 2).] The proton association for the intermediate events is constant over the full disk, although the total number of cases (11) is still not large. For the entire sun, however, the percentage association of the cutoff events (33 percent) begins to distinguish itself from that of the U-bursts (77 percent) and the intermediate events (73 percent). Although one cannot rule out the propagation effect as the cause of the weak proton association of the eastern hemisphere cutoff events vs that of the U-bursts, we note that the longitudinal distribution in this hemisphere of flare-bursts of the three spectral types (with clean proton circumstances) does not appear to favor either the U-bursts or the intermediate events vs the bursts with cutoff spectra (Figure 10). The median eastern hemisphere longitude for such events in each spectral class is as follows: U-bursts (E38, 29 events), intermediate events (E50, 4), and cutoff events (E29, 11). Thus in a consideration of the relationship of microwave peak-flux-density spectra to proton events of any size, the U-shaped spectrum is differentiated primarily from the cutoff spectrum that is deficient, and in many cases apparently lacking, in 200-MHz emission.

3.2 The U-Burst as a Forecast Tool

To derive a false alarm rate for the U-burst forecast tool, we counted as successes only those cases in which a U-burst was followed by a proton event with $J (> 10 \text{ MeV}) \geq 10 \text{ pr cm}^{-2} \text{ sec}^{-1} \text{ sr}^{-1}$.⁷ If we consider only western hemisphere events, we have 22 successes vs 21 false alarms for a false alarm rate of 4% percent (21/43). To determine the number of false alarms, we added the number of U-bursts without proton association to the number of U-bursts with clean and ambiguous/masked proton associations for which the characteristic of $\log (J / 10 \text{ MeV}) \leq 0$. We did not consider the eight masked or ambiguous cases for which the peak $> 10\text{-MeV}$ flux was above the prediction threshold. Technically, ambiguous cases with $J (> 10 \text{ MeV}) \geq 10 \text{ pr cm}^{-2} \text{ sec}^{-1} \text{ sr}^{-1}$ should be counted as

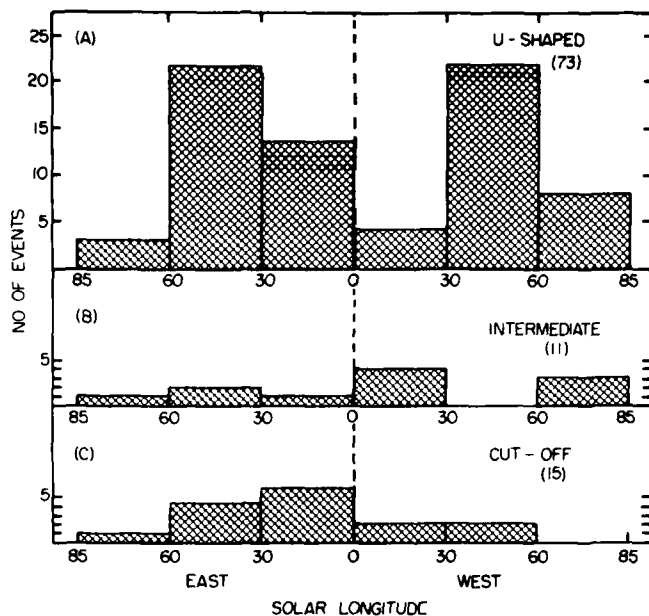


Figure 10. Histograms of the Longitudinal Distributions of the $\text{H}\alpha$ Flares Associated With the Large Microwave Bursts in Table 1 Distributed According to Spectral Classification: (a) U-Shaped, (b) Intermediate, and (c) Cutoff. Only those events with clean proton circumstances are shown

successes, but no such western hemisphere events occurred from 1965 to 1979, i.e., all eight events were masked. As a practical consideration, a "yes or no" forecast of a proton event above a given peak threshold is not very meaningful if that threshold is already exceeded, so we did not count these eight cases as false alarms. However, in this light, one might argue that the predictions for the U-bursts on 01 November 1968 or 04 and 07 August 1972, for example, should not be counted as successes but should similarly be disregarded since J (~ 10 MeV) was above threshold at the time of the prediction. Without belaboring the point further, we will let it suffice to say that during the period from 1965 to 1979, proton predictions for western hemisphere flare-bursts with U-shaped spectra would have resulted in a false alarm rate of ~ 50 percent for the current prediction threshold of J (~ 10 MeV) $\geq 10 \text{ pf cm}^{-2} \text{ sec}^{-1} \text{ sr}^{-1}$. Moreover, only 48 percent (22/46) of the large proton events listed in Table 2 would have been successfully forecast by the U-burst tool. Expanding the longitude range of flare-bursts for which predictions are made will increase both the fraction of events successfully forecast (success rate) and also the false alarm rate. Tarnstrom³⁶

³⁶Reference 36 will not be listed here. See References, page 50.

noted that for the period from 1966 to 1976, the performance of the U-burst forecast tool would have been optimized by issuing yes-no forecasts following U-bursts associated with flares located between E20 and W90. From the events in Tables 1 and 2, the values of the success and false alarm rates for this longitude range, actually E20 to W85, are 54 (25/46) and 56 percent (32/57) respectively. We note that even if the longitude range from E85 to W85, comprising all events in Table 2, is considered, the success rate is still only 61 percent (28/46) while the false alarm rate is 73 percent (75/103).

Since the U-burst forecast tool was originally developed for prediction of PCA events with ≥ 2.0 dB of 30-MHz riometer absorption,¹⁻³ corresponding to proton events with $J (> 10 \text{ MeV}) \geq 40 \text{ pr cm}^{-2} \text{ sec}^{-1} \text{ sr}^{-1}$,^{6,37} it is appropriate to consider how well it works for these larger events. Of the 46 events in Table 2, 29 (indicated by a 40 in column 10) had prompt components with $J (> 10 \text{ MeV}) \geq 40 \text{ pr cm}^{-2} \text{ sec}^{-1} \text{ sr}^{-1}$. Of these 29 events, 22 had U-shaped microwave spectra, 6 definitely did not have U-shaped spectra, (Table 2, Nos. 12, 19, 38, 43, 45, and 46), and we were unable to classify the remaining event (No. 35) from the data reported in SGD. Since event No. 19 on 07 March 1970 is considered to be a doubtful flare association,¹⁹ the percentage association of U-bursts with these large prompt proton events ranges from a worst case of 78 percent (22/29) to a best case of 82 percent (23/28) obtained by assuming No. 35 was a U-burst and disregarding No. 19 because of the parent flare ambiguity. It is interesting to note that four of the five large ($\geq 40 \text{ pr cm}^{-2} \text{ sec}^{-1} \text{ sr}^{-1}$) proton events (disregarding No. 19) without U-burst association occurred after 1976. The 22 U-bursts associated with the $J \geq 40$ proton events are not particularly distinguishable from the other U-bursts in Table 1. Although their peak flux densities at the centimeter and meter wavelengths tend to be larger, as might be expected, they range from values $< 1000 \text{ sfu}$ (Table 2, Nos. 2 and 34) to $> 20,000 \text{ sfu}$ (Nos. 6, 26, and 27) at 10 GHz, and from values $\leq 1000 \text{ sfu}$ (Nos. 3, 11, 25, 36, and 39) to $> 50,000 \text{ sfu}$ (Nos. 13 and 40) at 200 MHz. Moreover, the microwave spectra of these events encompass the full variety of shapes that are allowed by our definition of a U and include classic examples such as (Table 2) Nos. 2, 7, 13, 33, and 37 [see Figures 1(a), 1(d), and 2(b)] as well as less obvious cases such as Nos. 3, 24, 25, 32, and 34 [see Figures 3(b)-3(d)].

37. Juday, R. D., and Adams, G. W. (1969) Riometer measurements, solar proton intensities and radiation dose rates, Planet. Space Sci. 17:1313.

3.3 Radio Signatures of Major Proton Events

While Cliver et al¹⁹ demonstrated that a strong centimeter-wavelength emission peak (i.e., $S_p > 100$ sfu) is not a requirement for a prompt proton event with $J (\gtrsim 10 \text{ MeV}) \geq 10 \text{ pr cm}^{-2} \text{ sec}^{-1} \text{ sr}^{-1}$ to occur, it might be supposed that a prominent (≥ 1000 sfu) lower frequency (200 MHz) emission peak remains as a necessary observable for significant particle acceleration in (or escape from) flares. That this is not the case is shown in Figure 11, where a histogram of S_p (~ 200 MHz) for the events in Table 2 is presented. Even though we used the largest ~ 200 -MHz flux density peak reported by any observatory on patrol (and occurring at any time during the listed H α flare), eight events (seven, if we ignore 07 March 1970) had S_p (~ 200 MHz) ≤ 300 sfu. Thus neither the high frequency (~ 9 GHz) nor the low frequency (~ 200 MHz) branch of the classical (i.e., $S_p \gtrsim 1000$ sfu) U-burst appears to be a requirement for the occurrence of a large prompt proton event.

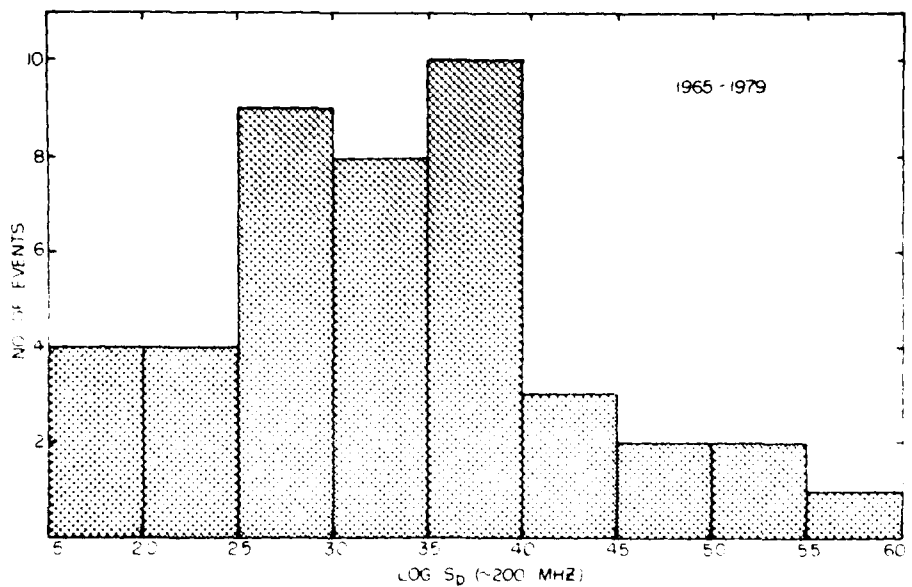


Figure 11. Histogram of the Reported Peak-Flux-Density at ~ 200 MHz for the Parent Flares of the Large [$J (\gtrsim 10 \text{ MeV}) \geq 10 \text{ pr cm}^{-2} \text{ sec}^{-1} \text{ sr}^{-1}$] Prompt Proton Events in Table 2 That Were Observed From 1965 to 1979. For each event we took the largest flux density reported by any observatory on patrol near 200 MHz (184 to 328 MHz) during the time of the associated H α disk ($85^\circ \text{E} \approx \phi \approx 85^\circ \text{W}$) flare. Note that several (8 of 46) of these events have relatively weak (≤ 300 sfu) emission at ~ 200 MHz.

Work by Pick-Gutmann,³⁸ Harvey,³⁹ and Castelli and Tarnstrom⁶ indicated that the integrated microwave flux-density (E_μ) obtained by taking the product of the burst mean flux-density and duration, might be an important parameter in regard to proton acceleration in flares.⁴⁰ In particular, the Pick-Gutmann and Castelli and Tarnstrom studies suggest that an integrated flux-density $E_\mu \gtrsim 10^{-17}$ Joules m⁻² Hz⁻¹ is a requirement (or threshold) for the observation of a polar cap absorption event. However, this value of E_μ is relatively small and can be achieved by a predominantly thermal burst (gradual rise and fall or post-burst increase) with a mean flux-density of 15 sfu and a duration of two hours. In fact, with the possible exception of the 21 August event,¹⁸ the weak impulsive phase proton events discussed by Cliver et al¹⁹ had values of $E_\mu > 10^{-17}$, primarily because of their long durations. Since there is no apparent close physical link between thermal microwave emission and non-thermal energetic protons,²² the concept of an integrated microwave flux-density threshold for proton acceleration in flares may be misleading.¹⁹

At this point, it is of interest to compare the U-shaped spectrum as an almost necessary or favorable condition for a significant proton event to occur with meter wavelength phenomena that have been linked to proton acceleration, specifically, Type II bursts^{20,21} and Type IV bursts.^{26,41,42} We find that Type IIs and Type IVs are associated with the events in Table 2 [and with the subset of events with $J (\sim 10 \text{ MeV}) \gtrsim 40 \text{ pr cm}^{-2} \text{ sec}^{-1} \text{ sr}^{-1}$] in the following percentages:

	J ($\sim 10 \text{ MeV}$)	
	$\sim 10 \text{ protons cm}^{-2} \text{ sec}^{-1} \text{ sr}^{-1}$	$\sim 40 \text{ protons cm}^{-2} \text{ sec}^{-1} \text{ sr}^{-1}$
Type II	80% (35/44)	85% (23/27)
Type IV	84% (36/43)	92% (24/26)
U-burst	65% (28/43)	81% (22/27)

-
- 38. Pick-Gutmann, M. (1961) Evolution des émissions radioélectriques solaires de Type IV et leur relation avec d'autres phénomènes solaires et géophysiques, Ann. Astrophys. 24:183.
 - 39. Harvey, G. A. (1965) 2800 megacycle per second radiation associated with Type II and Type IV solar radio bursts and the relation with other phenomena, J. Geophys. Res. 70:2961.
 - 40. Kundu, M. R., and Haddock, F. T. (1960) A relation between solar radio emission and polar cap absorption of cosmic noise, Nature 186:610.
 - 41. Bell, B. (1963) Type IV solar radio bursts, geomagnetic storms, and polar cap absorption (PCA) events, Smithsonian Contr. Ap. 8:119.
 - 42. Maxwell, A., Defouw, R. J., and Cummings, P. (1964) Radio evidence for solar corpuscular emission, Planet. Space Sci. 12:435.

The 07 March 1970 event was not included in these percentages; also excluded were Nos. 25 (Type II), 2 [see footnote (b) to Table 2] and 25 (Type IV), and 30 and 35 (U-burst). We emphasize that these percentage associations were obtained strictly on the basis of data reported in SGD and QBSA. A reexamination of the sweep frequency records might reveal possible Type II events [e.g., Maxwell,⁴³ and Böhme and Kruger⁴⁴ reported possible Type IIs for two flares in the August 1972 sequence (Table 1, Nos. 100 and 101) for which no Type II burst was initially reported in SGD; see also footnote (a) to Table 2]. Nevertheless, in view of the perceived link between Type II bursts and proton events, it is interesting that ~ 20 percent of the events in Table 2, comprising the largest proton events observed from 1965 to 1979, did not have obvious associated metric Type II bursts. We suggest two reasons for the absence of meter Type IIs in several large proton events. First, Robinson et al.⁴⁵ have recently shown that interplanetary Type II bursts, often associated with major particle events,⁴⁶ can have starting frequencies < 20 MHz and thus go undetected by ground-based sweep frequency patrols. Second, H. Ubarz (1984, private communication) informs us that a lack of dynamic range on the Weisenau spectrograph during this period (since corrected) could have resulted in a few Type IIs being masked by intense Type IV bursts.

The distribution of the durations of Type II bursts for the events in Table 2 is given in Figure 12(a). This distribution is similar to that obtained by Kahler²⁶ from a sample of Type II bursts associated with proton events of any size for the period from June 1973 to June 1980. (There are 17 common events in the two distributions.)²² In determining the percentage association for Type IVs, we did not consider reports of either continuum emission or Type I activity (beginning during the H α flare), both of which may be organically related to Type IV. The five events for which either of these emissions (but not Type IV) were reported are indicated in Table 2. The distribution of the durations of the Type IV events in Table 2 is given in Figure 12(b).

-
- 43. Maxwell, A. (1973) Dynamic spectra of four solar radio bursts during the period 1972 August 2-7, in Rep. UAG-28, pt. I, p. 255, H. E. Coffey, Ed., World Data Center A for Solar-Terr. Phys., Boulder, Colo.
 - 44. Böhme, A., and Kruger, A. (1973) On the type IV bursts of August 2, 4 and 7, 1972, in Rep. UAG-28, pt. I, p. 260, H. E. Coffey, Ed., World Data Center A for Solar-Terr. Phys., Boulder, Colo.
 - 45. Robinson, R. D., Stewart, R. T., and Cane, H. V. (1984) Properties of metre-wavelength solar bursts associated with interplanetary Type II emission, Sol. Phys. 91:159.
 - 46. Cane, H. V., and Stone, R. G. (1984) Type II solar radio bursts, interplanetary shocks, and energetic particle events, Astrophys. J. 282:339.

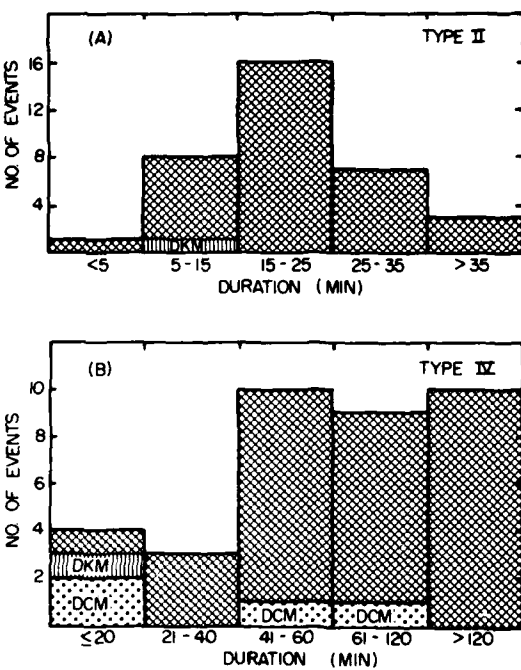


Figure 12. Histograms of the Durations of (a) Type II and (b) Type IV Emission for the Largest [$J (> 10 \text{ MeV}) \geq 10 \text{ pr cm}^{-2} \text{ sec}^{-1} \text{ sr}^{-1}$] Disk Flare ($85^\circ \text{E} \geq \phi \leq 85^\circ \text{W}$) Associated Prompt Proton Events That Occurred From 1965 to 1979. Events where only decimetric (DCM) or decametric (DKM) emissions were reported are indicated; all other events were observed at meter wavelengths

3.4 Microwave Spectral Class and Type II/IV Bursts

Because of the statistical relationships between U-bursts and proton events and between Type II/IV bursts and proton events, we have examined the associations of Type II/IV bursts with large microwave bursts of different peak-flux-density spectral types. The percentage associations of these phenomena are presented in Table 4, where it can be seen that the percentage associations of microwave bursts of different spectral class with Type II/IV bursts parallel their association with proton events ($85^\circ \text{E} \geq \phi \leq 85^\circ \text{W}$). We note that the microwave events with cutoff peak-flux-density spectra also appear to be deficient in Type III bursts. The statistical results in Table 4 are consistent with the current picture^{17, 47-49}

References 47 to 49 will not be listed here. See References, page 50.

Table 4. Association of Sweep Frequency Bursts and Proton Events With Peak-Flux-Density Spectral Classes

ASSOCIATED PHENOMENA SPECTRAL TYPE	TYPE III	TYPE II	TYPE IV	TYPE II&/or IV	FULL DISK PROTONS (CLEAN CASES)
U-SHAPED	(109) 93%	70%	73%	90%	(73) 77%
INTERMEDIATE	(18) 72%	61%	67%	78%	(11) 73%
CUT-OFF	(32) 34%	12%	19%	22%	(15) 33%
UNCLASSIFIED	(25) 80%	68%	68%	80%	(12) 67%

that the protons observed at Earth are accelerated at a shock front, and it appears that the U-bursts are preferentially related to protons, in contrast to cutoff events, because of their higher percentage association with Type II/IV events. We should be able to check this supposition directly by comparing the proton association of U-bursts (and cutoff events) that were accompanied by Type II and/or Type IV emission with those that were not. However, as can be seen from Table 4, the control group of U-bursts without Type II/IV association is relatively small. Only 11 U-bursts that lacked both Type II and Type IV associations are listed in Table 1. The spectra of three of these events, Nos. 19, 90, and 160, are shown in Figures 5(a), 5(c), and 2(c), respectively. Nine of these 11 events were associated with eastern hemisphere flares. For two of these nine events, Nos. 111 [-2 (M)] and 159 [-1 (M)], possible proton events were masked by small events in progress, while only one of the remaining seven events, No. 90 (-2), was associated with protons at the level (≥ -2) considered. Of the two western hemisphere events, one, No. 160 [-1 (M)], was masked, and one was unassociated. Thus only one of the eight clean control events (albeit seven of these from eastern hemisphere flares) was associated with a >10 -MeV proton event. For comparison, we note that 74 percent (23/31) of the clean eastern hemisphere U-bursts with Type II and/or Type IV bursts had proton association. The seven clean eastern hemisphere U-bursts without Type II/IV association had a median longitude of 45° , slightly less favorable than the 31 clean eastern hemisphere U-bursts with Type II/IV association, 38° . A consideration of the associations of cutoff events with and without

Type II/IV bursts and proton events is also hampered by small numbers although the results are consistent with the overall statistics presented in Table 4; three of the five clean cutoff events (E16 median longitude) with Type II/IV association were related to > 10 -MeV events as opposed to two of ten clean cutoff events (E20 median longitude) without Type II/IV association.

At this point, it is instructive to consider in greater detail some of the cutoff events that have proton association. For the event on 27 October 1968 [No. 29, $\log(J) = -1$], Tanaka (see Svestka and Simon,³⁰ Part 2), reports Type IV emission beginning at 1307 UT, ~ 30 min after the peak listed in Table 1 and near the start of a major [$Sp(5\text{ GHz}) = 860\text{ sfu}$] burst that we consider to be a secondary peak in an extended flare event. Similarly for the event on 16 November 1970 [No. 79, $\log(J) = -1$], the Type II/IV event begins at 0112 UT, ~ 20 min after the listed peak, but near the maximum of a significant [$Sp(9.4\text{ GHz}) = 1030\text{ sfu}$] burst apparently associated with the same $H\alpha$ flare. For both event Nos. 29 and 79, 200-MHz bursts were reported only in association with the later peak. These events indicate that it may be misleading to expect the spectrum of a single peak in a complex microwave burst to tell the entire story in regard to a flare's association with Type II/IV bursts and protons. For the above cases, it is tempting to speculate that the flares evolved from a compact to an open magnetic field structure.⁵⁰

One cutoff burst was associated with a large $J (> 10\text{ MeV})$ proton event. In the 15 November 1979 event [$\log(J) = 1$], the Type II/IV event began at 2147 UT, 4.2 min before the 10-GHz maximum. It can be seen from Svestka and Fritzová-Svestková's²¹ Figure 4 that such events are relatively rare.³⁹ This event also had a low ($\lesssim 2.7\text{ GHz}$) and apparently broad spectral maximum [Figure 9(d)]. In the published Penticton record of this event,¹² the listed peak is preceded by a smaller [$Sp(2.8\text{ GHz}) \sim 250\text{ sfu}$] peak at 2142 UT. Thus we tentatively identify the listed event as a secondary peak in a complex microwave Type IV event,⁵¹ and, as such, note that it may have a rather different nature than the other cutoff events in Table 1.

-
- 50. Pallavicini, R., Serio, S., and Vaiana, G. S. (1977) A survey of soft x-ray limb flare images: the relation between their structure in the corona and other physical parameters, *Astrophys. J.* **216**:108.
 - 51. Cliver, E. W. (1983) Secondary peaks in solar microwave outbursts, *Sol. Phys.* **84**:347.

3.5 Timing of Type II Burst and 200-MHz Peak

Given the statistical associations between Type IIs, protons, and U-bursts (and the relative deficiency of Type II emission and proton association in the cut-off events), it seems logical to ask if the shock wave observed via the Type II burst, and presumably accelerating the protons, might in some way account for the low frequency branch of the U, particularly the high fluxes often observed near 200 MHz. There are two possible ways that the Type II burst could account for, or contribute to, the 200-MHz radiation. First the Type II itself is generally an intense emission with flux densities ranging from ~ 50 to several thousand sfu.²⁴ For those events with relatively high starting frequencies, emission at the second harmonic would be in the 200-MHz range and thus might contribute to the low frequency branch of the U. About one-third of Type II bursts have fundamental starting frequencies > 100 MHz,⁵² and about 60 percent of Type IIs exhibit harmonic structure.²⁴ A second possible way in which a shock wave might contribute to the 200-MHz emission that often comprises the low frequency branch of the U is through the flare continuum emission designated as FC II by Robinson and Smerd.⁵³ This emission follows the Type II burst at any frequency and is thought to be due to shock accelerated electrons trapped in a large scale magnetic loop.⁵⁴ To see if either the Type II or FC II could contribute to the 200-MHz emission in U-bursts, we determined whether the associated (if any) Type II burst was in progress at the time of the 200-MHz peak (within the sliding five-minute window) for each of the U-bursts in Table 1. We counted as concomitant those cases in which Type II bursts were in progress or began within ≤ 0.5 min after the average peak time at 200 MHz. Since the low frequency branch of the U-shaped spectrum may be due to flash phase accelerated electrons, we also looked to see if a Type III burst was in progress at the time of the low frequency maximum (Xs in column 21 of Table 1), since these emissions are a characteristic component of the impulsive phase.⁵⁵ (Type IV emission was in progress at the time of the 200-MHz peak for about half of the U-bursts, but since flare continuum can also have

-
- 52. Maxwell, A., and Thompson, A. R. (1962) Spectral observations of radio bursts, II: slow drift bursts and coronal streamers, *Astrophys. J.* 135:138.
 - 53. Robinson, R. D., and Smerd, S. F. (1975) Solar flare continua at the metre wavelengths, *Proc. ASA* 2:374.
 - 54. Robinson, R. D. (1978) A study of solar flare continuum events observed at metre wavelengths, *Aust. J. Phys.* 31:533.
 - 55. Kane, S. R. (1974) Impulsive (flash) phase of solar flares: Hard x-ray microwave, euu and optical observations, in *Coronal Disturbances*, Proc. of IAU Symp. No. 57, p. 105, G. Newkirk, Jr., Ed., D. Reidel Pub. Co., Dordrecht, Holland.

a component attributed to primary phase electrons,⁵⁴ an ambiguity exists.) The results of the timing comparisons were as follows:

In Progress at
Time of 200-MHz Peak*
(%)

Type II only	19
Type II and Type III	30
Type III only	44
Neither	7

*Sample size = 103 events. For 10 events the reported 200-MHz maximum either fell well outside the five-minute window, observations were not made at 200 MHz, or sweep frequency observations were not available.

From these statistics, it can be seen that the FC II and Type II emission could contribute to the peak 200-MHz emission in U-bursts in at most ~ 50 percent of the cases, assuming that the starting frequency of the fundamental Type II emission is $\lesssim 100$ MHz. For 21 U-bursts in Table 1 that occurred during Culgoora observing hours, we were able to check the starting frequencies of the associated Type IIs from a compilation by Robinson et al.⁵⁶ Harmonic emission started at $f \gtrsim 200$ MHz for only about half of these events ($11/21 = 52$ percent),⁵² although for those events where the Type II was in progress at the time of the 200-MHz peak, harmonic emission began at $f \gtrsim 200$ MHz in 71 percent ($10/14$) of the cases. (We note in passing that only one of the 11 20th solar cycle U-bursts had starting harmonic frequencies $\gtrsim 200$ MHz vs 10 of 10 from the 21st solar cycle.) For 51 percent of the U-bursts in our sample, a Type II was either not observed, ended prior to, or began ≥ 0.5 min after the peak of the 200-MHz emission. A comparison of the peak 200-MHz flux densities of these U-bursts (the 51 percent) with those of the Type II coincident events revealed no marked differences between the two distributions. The median 200-MHz flux value of the Type II coincident events (3400 sfu) is larger, as might be expected, but the median value for the non-coincident events (2000 sfu) is also well above the minimum value ($\gtrsim 1000$ sfu) required for the classical U-burst. Since the 200-MHz peak is coincident with

⁵⁶ Robinson, R. D., Tuxford, J. M., Sheridan, K. V., and Stewart, R. T. (1983) A catalogue of major metre-wavelength solar events recorded by the DAPTO and Culgoora solar radio observatories (1961 - 1981), Proc. ASA 5:84.

Type III emission for 74 percent of the U-bursts examined, it appears that flash phase electrons are primarily responsible for the low frequency branch of the U-shaped spectrum.

4. DISCUSSION

4.1 Summary

From this study of the peak-flux-density spectra of nearly 200 large [S_p (≥ 2 GHz) ≥ 800 sfu] microwave bursts and their associated proton and sweep frequency emissions, we have found the following:

(1) There appear to be two basic peak-flux-density spectral types: (a) U-shaped, with two maxima ≥ 800 sfu in the range from 200 MHz to ≥ 10 GHz (59 percent of all events) and (b) cutoff, with a spectral maximum ≥ 800 sfu at $f \geq 2$ GHz and S_p (200 MHz) < 100 sfu (18 percent). Nine percent of the events had what we termed intermediate spectra with a spectral maximum ≥ 800 sfu at $f \geq 2$ GHz and 100 sfu $\leq S_p$ (200 MHz) < 800 sfu. We were unable to classify 15 percent of the events in our data sample.

(2) If the current NOAA proton prediction threshold of J (> 10 MeV) ≥ 10 protons $\text{cm}^{-2} \text{ sec}^{-1} \text{ sr}^{-1}$ had been in effect during the period covered by our data base (1965-1979), the U-burst "yes or no" proton event forecast tool would have had a false alarm rate of ~ 50 percent and would have failed to provide a warning for ~ 50 percent of the significant prompt proton flares attributable to disk flares during this period. These figures apply if proton event warnings had been issued only following U-bursts associated with western hemisphere flares. If warnings had been made following U-bursts from anywhere on the sun ($85^\circ E \geq \phi \leq 85^\circ W$), the false alarm rate would have been 73 percent, and 39 percent of the significant proton events would not have been predicted by this method.

(3) The associations of flare-bursts ($85^\circ E \geq \phi \leq 85^\circ W$) of different peak-flux-density spectral type with Type II and/or Type IV bursts and with > 10 -MeV proton events of any peak intensity (≥ 0.01 pr $\text{cm}^{-2} \text{ sec}^{-1} \text{ sr}^{-1}$) are as follows: U-shaped - Type II/IV (90 percent of U-bursts are associated with Type II/IV events), protons (77 percent); intermediate - Type II/IV (78 percent), protons (73 percent); cutoff - Type II/IV (22 percent), protons (33 percent).

(4) In 74 percent of the microwave bursts with U-shaped spectra, the 200-MHz emission peak occurred during a Type III event. For 49 percent of the U-bursts, a Type II was in progress during, or began ≤ 0.5 min after, the peak 200-MHz emission.

(5) Several (8 of 46) of the proton events with $J (> 10 \text{ MeV}) \geq 10 \text{ protons cm}^{-2} \text{ sec}^{-1} \text{ sr}^{-1}$ (1965 - 1979) originated in visible hemisphere flares with relatively weak ($\text{Sp} \leq 300 \text{ sfu}$) associated 200-MHz emission. . .

4.2 The U-Burst as a Prediction Tool

The pessimistic picture of the U-shaped peak-flux-density spectrum as a proton prediction tool that we have presented in this study contrasts with that of earlier studies.⁵ We point out, however, that the differences in our results stem primarily from: (1) the use of a lower event prediction threshold than was previously used,⁷ i.e., $J (> 10 \text{ MeV}) < 10 \text{ pr cm}^{-2} \text{ sec}^{-1} \text{ sr}^{-1}$ vs $J \sim 40 \text{ pr cm}^{-2} \text{ sec}^{-1} \text{ sr}^{-1}$,^{2,6} and (2) the observation after 1976, the final year considered in studies by Castelli and Barron⁵ and Castelli and Tarnstrom,⁶ of several (Table 2, Nos. 38, 43, 45, and 46) large ($J \sim 40$) proton events that originated in flares with non-U microwave spectra. Despite differences in the basic approach (and the classification of several individual events) between ours and the earlier studies, our results pertaining to the U-burst as a forecast tool are in general agreement with those of Castelli and his co-workers for the prediction threshold and the time period they considered. Moreover, until a more reliable early indicator of proton acceleration/escape in flares is identified, the U-burst tool (or variants⁵⁷) will most likely continue to be used in combination with $H\alpha$ and sweep-frequency radio signatures at solar forecast centers.

Nevertheless, the recent observation of four large ($J \gtrsim 40$) proton events [two of which (Table 2, Nos. 43 and 45) were ground level events] associated with microwave bursts with non-U spectra underscores suspicions raised in other studies^{19, 22, 26} that the U-shaped spectrum may not have a strong physical connection with the process by which the protons observed at Earth are accelerated. Even for the $J \gtrsim 40$ events that were preceded in ~80 percent of the cases by bursts with U-shaped spectra, the wide variation in spectral shape among events like 06 April 1971 [Table 1, No. 86, and Figure 3(c)] with a large decimetric peak and weak 200-MHz emission, events like 07 July 1966⁵⁸ and 24 January 1971 [No. 85, Figure 3(b)] that are classified as U-bursts because of relatively sharp spectral variations in the decimetric range, and the more classic types such as Nos. 5 and 131 [Figures 1(a) and 1(d)], makes it difficult to embrace U-bursts as

-
- 57. Akinyan, S. T., Chertok, I. M., and Fomichev, V. V. (1979) Quantitative forecasts of solar protons based on solar flare radio data, in Solar Terrestrial Predictions Proceedings, vol. 3, D-14, R. F. Donnelly, Ed., National Oceanic and Atmospheric Administration, Boulder, Colo.
 - 58. Svestka, Z. (1976) Solar Flares, D. Reidel Pub. Co., Hingham, Mass., p. 193.

a special class of microwave bursts that are somehow uniquely related to interplanetary proton events. We attribute the high percentage of association (31 of 34 western hemisphere cases) of these phenomena to the fact that U-bursts are generally (90 percent of the time) accompanied by Type II and/or Type IV bursts indicative of a second stage process involving a shock wave.

4.3 The Low Frequency Branch of the U-Shaped Spectrum

Kundu and Vlahos⁵⁹ have suggested that the U-shaped spectrum is a reflection of nothing more than the fact that there are two different sources of burst radiation, one for centimeter wavelengths and one for decimeter wavelengths, with different electron energy distributions and different magnetic fields. In this study we asked whether the two emission maxima might not also reflect different acceleration processes for the radiating electrons that give rise to the separate branches of the U-shaped spectrum. In particular we entertained a picture in which a shock wave might account for the low frequency (~ 200 MHz) branch of the U, either through emission from the second harmonic of the Type II burst or through flare continuum (FC II) radiation,⁵⁴ in those cases where the starting frequency of the fundamental Type II burst is $\gtrsim 100$ MHz. We found that this picture cannot obtain in general since a Type II burst was in progress at the time of the low frequency maximum (nominally at 200 MHz) for only about half of the U-bursts in our sample. This conclusion is based on the assumption that the shock either does not exist or is incapable of accelerating electrons prior to the occurrence of a Type II burst. In 74 percent of the cases, the peak 200-MHz emission in U-bursts occurred at the time of reported Type III emission, suggesting that the low frequency branch of the U is primarily due to radiation from flash phase electrons. In fact, since both the starting frequency and intensity of Type III emission can be expected to increase with the size of the associated microwave (hard x-ray) burst,⁶⁰ it seems likely that, for the U-bursts, the low frequency branch is often due to the Type III burst itself. In this context we note that, in addition to having relatively weak proton and Type II associations, the cutoff events in our sample were also deficient in Type III emission.

59. Kundu, M. R., and Vlahos, L. (1982) Solar microwave bursts - a review, *Space Science Reviews* 32:405.

60. Kane, S. R. (1981) Energetic electrons, type III radio bursts, and impulsive solar flare x-rays, *Astrophys. J.* 247:1113.

4.4 U-Bursts and the Big Flare Syndrome

The large [Sp (≥ 2 GHz) ≥ 800 sfu] microwave bursts examined in the study tend to have U-shaped peak-flux-density spectra (59 percent, 113/193) and to be associated with Type II/IV bursts (76 percent, 139/184) and > 10 -MeV proton events (69 percent, 77/111). However, the small number of events with U-shaped spectra that lacked both Type II and Type IV emission were poorly associated with interplanetary protons. This argues that the Type II/IV burst is the critical observable for particle acceleration and not the U-shaped spectrum. The fact that the statistical association of the cutoff bursts with proton events parallels their associations with Type II/IV bursts provides additional support for this contention. In addition, we note that for the majority of the U-bursts in our sample, the high fluxes often observed near 200 MHz appear to be more closely related to Type III emission than to the shock wave (Type II burst) that is presumably accelerating the protons. Thus we conclude that the U-shaped spectrum, at both high (~ 10 GHz) and low (~ 200 MHz) frequencies, is primarily an impulsive phase phenomenon and that the observed statistical U-burst/proton association is probably due to the Big Flare Syndrome²² rather than the result of a direct physical connection between these two phenomena. The observation that the cutoff events are deficient in Type III as well as Type II emission relative to the U-bursts, however, suggests that a less direct or "once-removed" connection may exist between the U-shaped spectrum and proton acceleration in that the probability of shock formation (Type II/protons) in these large flares apparently increases in more open magnetic field structures (Type III/U-burst).

4.5 Impulsive Phase Proton Acceleration

Forrest⁶¹ and Forrest and Chupp⁶² have recently presented γ -ray evidence indicating that ions are accelerated along with electrons in the impulsive phase of all flares. However, Cliver et al⁶³ have shown that the correlation between γ -ray line fluences and interplanetary proton fluxes is poor. This leaves open the possibility that the ions observed at the sun via gamma ray line emission are accelerated by a different process than the bulk of the protons detected at 1 a.u. In particular, we favor a picture, as advocated above, in which the protons observed at Earth are accelerated in a second stage process involving a shock wave.^{64, 65}

Cane et al⁶⁵ have shown that interplanetary particles accelerated during the flare impulsive phase have a narrower cone of emission/propagation than those presumably accelerated by a shock wave. In this context we note that nine of the

References 61 to 65 will not be listed here. See References, page 50.

11 U-bursts lacking Type II/IV association originated in eastern hemisphere flares, making it difficult to observe at Earth any impulsively accelerated protons that may have escaped from the sun in these events.

4.6 Proton Flares With Weak 200-MHz Emission

As a final comment, we note that in the largest disk flare associated proton events ($J > 10$) observed from 1965 to 1979, the 200-MHz emission was often relatively weak, ≤ 300 sfu in eight of 46 cases. While either Type II or Type IV emission was lacking in a comparable number of cases, the identification of these sweep frequency events is more subject to interpretation, and it is possible that upon reexamination of the original records, the missing phenomenon might be noted. The 200-MHz records should be less ambiguous, however, and we considered the highest flux density reported by any observatory during the associated $H\alpha$ flare. Moreover, inspection of Table 2 reveals that several of even the events with $J (> 10 \text{ MeV}) \gtrsim 40 \text{ pr cm}^{-2} \text{ sec}^{-1} \text{ sr}^{-1}$ had relatively weak emission at $f \sim 200 \text{ MHz}$, the lowest frequency currently monitored on a 24-hr per day basis by the ground based solar radio patrol. Thus the low-frequency ($\sim 200 \text{ MHz}$) branch of the classical (i.e., $S_p \gtrsim 1000 \text{ sfu}$) U-burst does not appear to be a requirement for the occurrence of a large prompt proton event. The lack of a radio response at this frequency commensurate with the observed intensities of these large proton events indicates that, for certain flares, a radio signature of particle acceleration/escape may only exist at lower frequencies ($< 200 \text{ MHz}$) as was the case for the 04 October 1965 proton flare,^{66,67} the GLE-associated flare on 21 August 1979,¹⁸ and the eruptive filament event on 05 December 1981.⁶⁸

-
- 66. Böhme, A. (1972a) The time behavior of the continua during the initial stage of type IV bursts, Sol. Phys. 24:457.
 - 67. Böhme, A. (1972b) Spectral behaviour and proton effects of the type IV broad band continua, Sol. Phys. 25:478.
 - 68. Kahler, S. W., Cliver, E. W., Cane, H. V., McGuire, R. E., Stone, R. G., and Sheeley, Jr., N. R. (1986) Solar filament eruptions and energetic particle events, Astrophys. J. (in press).

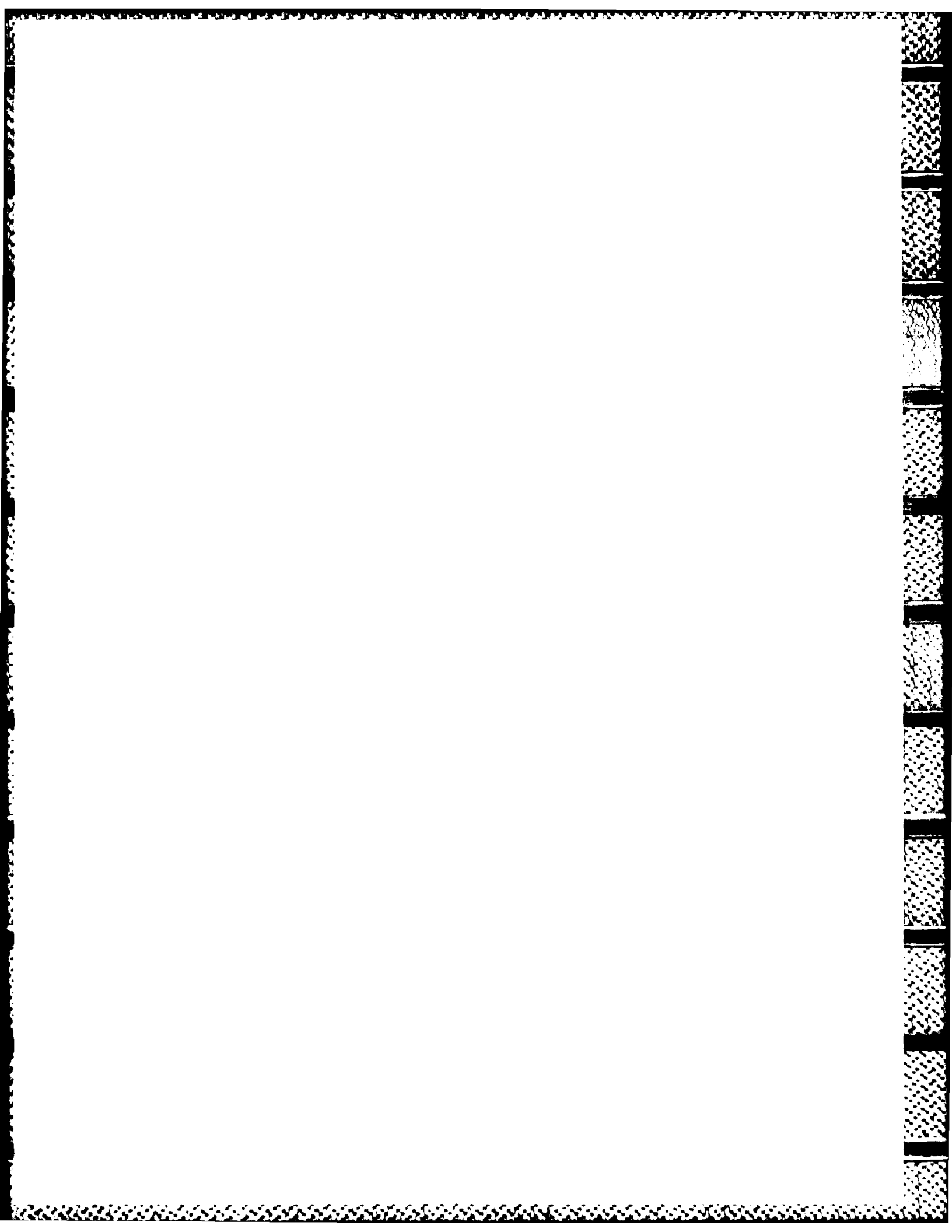
References

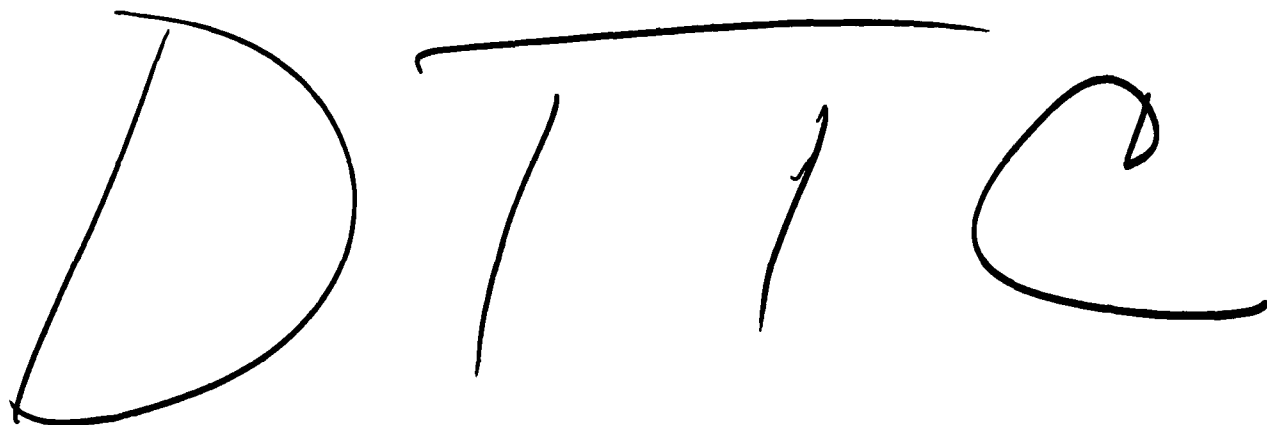
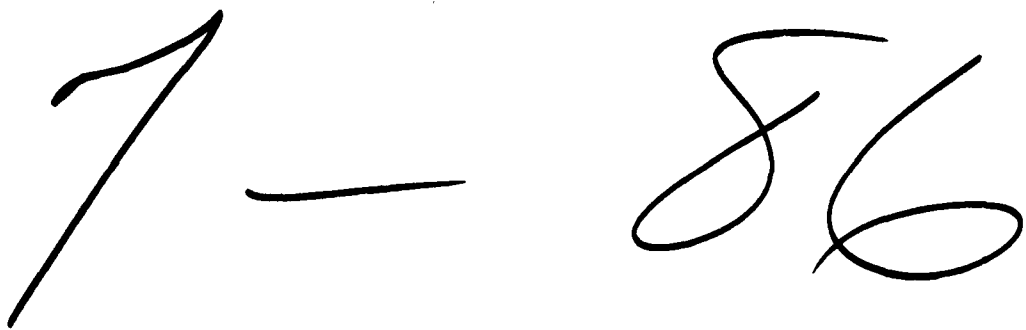
1. Castelli, J. P., Aarons, J., and Michael, G. A. (1967) Flux density measurements of radio bursts of proton-producing flares and nonproton flares, J. Geophys. Res. 72:5491.
2. Castelli, J. P. (1968) Observation and Forecasting of Solar Proton Events, AFCRL-68-0104, AD 669347.
3. O'Brien, W. E. (1970) The Prediction of Solar Proton Events Based on Solar Radio Emission, AFCRL-70-0425, AD 875024.
4. Castelli, J. P., and Guidice, D. A. (1972a) On the Classification, Distribution, and Interpretation of Solar Microwave Burst Spectra and Related Topics, AFCRL-72-0049, AD 741750.
5. Castelli, J. P., and Barron, W. R. (1977) A catalog of solar radio bursts 1966 - 1976 having spectral characteristics predictive of proton activity, J. Geophys. Res. 82:1275.
6. Castelli, J. P., and Tarnstrom, G. L. (1978) A Catalog of Proton Events 1966 - 1976 Having Non-Classical Solar Radio Burst Spectra, AFGL-TR-78-0121, AD A060816.
7. Heckman, G. (1979) Predictions of the space environment services center, in Solar Terrestrial Predictions Proceedings, vol. 1, p. 322, R. F. Donnelly, Ed., National Oceanic and Atmospheric Administration, Boulder, Colo.
8. Cliver, E. W., Secan, J. A., Beard, E. D., and Manley, J. A. (1978) Prediction of solar proton events at the Air Force Global Weather Central's space environmental forecasting facility, in Effect of the Ionosphere on Space and Terrestrial Systems, Conf. Proc., J. M. Goodman, Ed., U. S. Government Printing Office, Washington, D. C.
9. Thompson, R. L., and Secan, J. A. (1979) Geophysical forecasting at AFGWC, in Solar Terrestrial Predictions Proceedings, vol. 1, p. 350, R. F. Donnelly, Ed., National Oceanic and Atmospheric Administration, Boulder, Colo.

10. Castelli, J. P., Aarons, J., Guidice, D. A., and Straka, R. M. (1973) The solar radio patrol network of the USAF and its application, Proc. IEEE 61:1307.
11. Guidice, D. A., Cliver, E. W., Barron, W. R., and Kahler, S. (1981) The Air Force RSTN system, Bull. AAS 13:553.
12. Solar Geophysical Data, National Oceanic and Atmospheric Administration, Boulder, Colo.
13. Quarterly Bulletin of Solar Activity, International Astronomical Union, Eidgen. Sternwarte, Zurich.
14. Castelli, J. P., and Guidice, D. A. (1972b) The radio event associated with the polar cap absorption event of 2 November 1969, in Proc. of COSPAR Symposium on Particle Event of November 1969, p. 27, J. C. Ulwick, Ed., AFCRL-72-0474, AD 763081.
15. Wild, J. P., Smerd, S. F., and Weiss, A. A. (1963) Solar bursts, Ann. Rev. Astron. Astrophys. 1:291.
16. de Jager, C. (1969) Solar flares; properties and problems, in Proc. of COSPAR Symposium on Solar Flares and Space Research, p. 1, C. de Jager and Z. Svestka, Eds., North Holland Pub. Co., Amsterdam, Holland.
17. Lin, R. P., and Hudson, H. S. (1976) Non-thermal processes in large solar flares, Sol. Phys. 50:153.
18. Cliver, E. W., Kahler, S. W., Cane, H. V., Koomen, M. J., Michels, D. J., Howard, R. A., and Sheeley, Jr., N. R. (1983b) The GLE-associated flare of 21 August, 1979, Sol. Phys. 89:181.
19. Cliver, E. W., Kahler, S. W., and McIntosh, P. S. (1983c) Solar proton flares with weak impulsive phases, Astrophys. J. 264:699.
20. Lin, R. P. (1970) The emission and propagation of 40 keV solar flare electrons. I: the relationship of 40 keV electron to energetic proton and relativistic electron emission by the sun, Sol. Phys. 12:266.
21. Svestka, Z., and Fritzova-Svestkova, L. (1974) Type II radio bursts and particle acceleration, Sol. Phys. 36:417.
22. Kahler, S. W. (1982a) The role of the big flare syndrome in correlations of solar energetic proton fluxes and microwave burst parameters, J. Geophys. Res. 87:3439.
23. Bailey, D. K. (1964) Polar cap absorption, Planet. Space Sci. 12:495.
24. Kundu, M. R. (1965) Solar Radio Astronomy, Interscience Publishers, New York, New York.
25. Kai, K. (1968) Evolutional features of solar microwave type IV bursts, Pub. Astron. Soc. Japan 20:140.
26. Kahler, S. W. (1982b) Radio burst characteristics of solar proton flares, Astrophys. J. 261:710.
27. Tanaka, H., Castelli, J. P., Covington, A. E., Kruger, A., Landecker, T. L., and Tlamicha, A. (1973) Absolute calibration of solar radio flux density in the microwave region, Sol. Phys. 29:243.
28. Zirin, H., and Tanaka, K. (1973) The flares of August 1972, Sol. Phys. 32:173.
29. Roelof, E. C., Dodson, H. W., and Hedeman, E. R. (1983) Dependence of radio emission in large H α flares 1967 - 1970 upon the orientation of the local solar magnetic field, Sol. Phys. 85:339.

30. Svestka, Z., and Simon, P., Eds. (1975) Catalog of Solar Particle Events, 1955 - 1969, D. Reidel Pub. Co., Dordrecht, Holland.
31. Dodson, H. W., Hedeman, E. R., and Mohler, O. C. (1977) Survey and Comparison of Solar Activity and Energetic Particle Emission in 1970, AFGL-TR-77-0222, AD A048479.
32. Dodson, H. W., Hedeman, E. R., and Mohler, O. C. (1978) Solar and Geophysical Associations With the Principal Energetic Particle Events in 1971 and 1972, AFGL-TR-78-0266, AD A065260.
33. van Hollebeke, M. A. I., Ma Sung, L. S., and McDonald, F. B. (1975) The variation of solar proton energy spectra and size distribution with helio-longitude, Sol. Phys. 41:189.
34. Smart, D. F., and Shea, M. A. (1971) Solar proton event classification system, Sol. Phys. 16:484.
35. Reinhard, R., and Wibberenz, G. (1974) Propagation of flare protons in the solar atmosphere, Sol. Phys. 36:473.
36. Tarnstrom, G. L. (1978) Terrestrial proton events and solar radio bursts with U-shaped spectra, unpublished report.
37. Juday, R. D., and Adams, G. W. (1969) Riometer measurements, solar proton intensities and radiation dose rates, Planet. Space Sci. 17:1313.
38. Pick-Gutmann, M. (1961) Evolution des émissions radioélectriques solaires de Type IV et leur relation avec d'autres phénomènes solaires et géophysiques, Ann. Astrophys. 24:183.
39. Harvey, G. A. (1965) 2800 megacycle per second radiation associated with Type II and Type IV solar radio bursts and the relation with other phenomena, J. Geophys. Res. 70:2961.
40. Kundu, M. R., and Haddock, F. T. (1960) A relation between solar radio emission and polar cap absorption of cosmic noise, Nature 186:610.
41. Bell, B. (1963) Type IV solar radio bursts, geomagnetic storms, and polar cap absorption (PCA) events, Smithsonian Contr. Ap. 8:119.
42. Maxwell, A., Defouw, R. J., and Cummings, P. (1964) Radio evidence for solar corpuscular emission, Planet. Space Sci. 12:435.
43. Maxwell, A. (1973) Dynamic spectra of four solar radio bursts during the period 1972 August 2-7, in Rep. UAG-28, pt. I, p. 255, H. E. Coffey, Ed., World Data Center A for Solar-Terr. Phys., Boulder, Colo.
44. Böhme, A., and Kruger, A. (1973) On the type IV bursts of August 2, 4 and 7, 1972, in Rep. UAG-28, pt. I, p. 260, H. E. Coffey, Ed., World Data Center A for Solar-Terr. Phys., Boulder, Colo.
45. Robinson, R. D., Stewart, R. T., and Cane, H. V. (1984) Properties of metre-wavelength solar bursts associated with interplanetary Type II emission, Sol. Phys. 91:159.
46. Cane, H. V., and Stone, R. G. (1984) Type II solar radio bursts, interplanetary shocks, and energetic particle events, Astrophys. J. 282:339.
47. Kahler, S. W., Hildner, E., and van Hollebeke, M. A. I. (1978) Prompt solar proton events and coronal mass ejections, Sol. Phys. 57:429.
48. Cliver, E. W., Kahler, S. W., Shea, M. A., and Smart, D. F. (1982) Injection onsets of ~ 2 GeV protons, ~ 1 MeV electrons, and ~ 100 keV electrons in solar cosmic ray flares, Astrophys. J. 260:362.
49. Mason, G. M., Gloeckler, G., and Hovestadt, D. (1984) Temporal variations of nucleonic abundances in solar flare energetic particle events. II. Evidence for large scale shock acceleration, Astrophys. J. 280:902.

50. Pallavicini, R., Serio, S., and Vaiana, G. S. (1977) A survey of soft x-ray limb flare images: the relation between their structure in the corona and other physical parameters, *Astrophys. J.* 216:108.
51. Cliver, E. W. (1983) Secondary peaks in solar microwave outbursts, *Sol. Phys.* 84:347.
52. Maxwell, A., and Thompson, A. R. (1962) Spectral observations of radio bursts, II: slow drift bursts and coronal streamers, *Astrophys. J.* 135:138.
53. Robinson, R. D., and Smerd, S. F. (1975) Solar flare continua at the metre wavelengths, *Proc. ASA* 2:374.
54. Robinson, R. D. (1978) A study of solar flare continuum events observed at metre wavelengths, *Aust. J. Phys.* 31:533.
55. Kane, S. R. (1974) Impulsive (flash) phase of solar flares: Hard x-ray microwave, euu and optical observations, in *Coronal Disturbances*, Proc. of IAU Symp. No. 57, p. 105, G. Newkirk, Jr., Ed., D. Reidel Pub. Co., Dordrecht, Holland.
56. Robinson, R. D., Tuxford, J. M., Sheridan, K. V., and Stewart, R. T. (1983) A catalogue of major metre-wavelength solar events recorded by the DAPTO and Culgoora solar radio observatories (1961 - 1981), *Proc. ASA* 5:84.
57. Akinyan, S. T., Chertok, I. M., and Fomichev, V. V. (1979) Quantitative forecasts of solar protons based on solar flare radio data, in *Solar Terrestrial Predictions Proceedings*, vol. 3, D-14, R. F. Donnelly, Ed., National Oceanic and Atmospheric Administration, Boulder, Colo.
58. Svestka, Z. (1976) *Solar Flares*, D. Reidel Pub. Co., Hingham, Mass., p. 193.
59. Kundu, M. R., and Vlahos, L. (1982) Solar microwave bursts - a review, *Space Science Reviews* 32:405.
60. Kane, S. R. (1981) Energetic electrons, type III radio bursts, and impulsive solar flare x-rays, *Astrophys. J.* 247:1113.
61. Forrest, D. J. (1983) Solar γ -ray lines, *Am. Inst. of Physics Conf. Proc.* 101:3.
62. Forrest, D. J., and Chupp, E. L. (1983) Simultaneous acceleration of electrons and ions in solar flares, *Nature* 305:5932.
63. Cliver, E. W., Forrest, D. J., McGuire, R. E., and von Rosenvinge, T. T. (1983a) Nuclear gamma rays and solar proton events, *Conf. Pap. Int. Cosmic Ray Conf.* 18th 10:342.
64. Kahler, S. W., Sheeley, Jr., N. R., Howard, R. A., Koomen, M. J., Michels, D. J., McGuire, R. E., von Rosenvinge, T. T., and Reames, D. V. (1984) Associations between coronal mass ejections and solar energetic proton events, *J. Geophys. Res.* 89:9683.
65. Cane, H. V., McGuire, R. E., and von Rosenvinge, T. T. (1985) Two classes of energetic particle events associated with impulsive and long duration soft x-ray flares, *Astrophys. J.* (in press).
66. Böhme, A. (1972a) The time behavior of the continua during the initial stage of type IV bursts, *Sol. Phys.* 24:457.
67. Böhme, A. (1972b) Spectral behaviour and proton effects of the type IV broad band continua, *Sol. Phys.* 25:478.
68. Kahler, S. W., Cliver, E. W., Cane, H. V., McGuire, R. E., Stone, R. G., and Sheeley, Jr., N. R. (1986) Solar filament eruptions and energetic particle events, *Astrophys. J.* (in press).



DTTC7 - 86